Determining Differential Expression Patterns of MicroRNAs in Mammalian Skin by *In Situ* Hybridization

By: Emily Rose Shangraw

Molecular, Cellular, and Developmental Biology

April, 1, 2011

Advisor:

Rui Yi

Committee Members:

Nancy Guild,

Christine Kelly,

and Elspeth Dusinberre

Abstract:

MicroRNAs are small non-coding RNAs that regulate gene expression post-transcriptionally (Bartel, 2009). Several different microRNAs have been implicated in regulatory pathways of skin morphogenesis, stem cells, skin cancer, and other skin diseases. A subset of microRNAs have been found to be differentially expressed in distinct skin lineages, namely epidermis and hair follicle (Yi et al., 2006). Characterization of the spatial and temporal expression patterns of these microRNAs can provide a basis to investigate their functions during development as well as in skin diseases including skin cancer. During my thesis study, I employed *in situ* hybridization to characterize the differential expression of four discrete microRNAs: miR-203, miR-143, miR-125b, and miR-205 in mammalian skin. My results demonstrated that miR-203 is highly expressed in differentiating skin lineages, miR-143 is enriched in the transient amplifying cells in hair follicle matrix, miR-125b and miR-205 are enriched in skin stem cells. I also cloned three regions upstream of miR-205 and analyzed their promoter activity in cultured keratinocytes. Together, my study shows that miRNAs are differentially expressed in distinct skin lineages and provides a basis to analyze their functions in the future.

Table of Contents:

Chapter 1: Background

Section 1: Importance of MicroRNA and Mammalian Skin Models

Section 2: Importance of Stem Cell Regulation

Section 3: MicroRNA Biogenesis and Function

Section 4: Skin Cell Lineages

Section 5: Hair Follicle Cycling

Section 6: MicroRNAs in the Skin

Section 7: Previous Knowledge and Published Data

Section 8: Experimental Plan

Chapter 2: Materials and Methods

Section 1: In Situ Hybridization

Section 2: Real Time Quantitative Polymerase Chain Reaction (RT- qPCR)

Section 3: Quantitative PCR to determine microRNA expression levels

Section 4: Luciferase Assay

Section 5: Molecular Cloning

Chapter 3: Results

Section 1:miR-203

A. NBT/BCIP

B. Fluorescent In Situ Hybridization

Section 2: miR-143

A. NBT/BCIP

B. Fluorescent In Situ Hybridization

C. Embryonic Tissue Expression

Section 3: miR-125b

A. NBT/BCIP

Section 4: miR-205

A. NBT/BCIP

B. Confocal Images

C. Embryonic Exploration

D. RT-qPCR

Section 5: Luciferase Assay

A. Construct A

B. Construct B

C. Construct C

D. 293T Luciferase Assay

Chapter 4: Discussion

Section 1: In Situ Hybridization

A. miR-203 Expression patterns

B. miR-143 Expression patterns

C. miR-125b Expression patterns

D. miR-205 Expression patterns

E. miR-205 RT-qPCR

Section 2: Luciferase Assay

Section 3: Conclusions

Chapter 5: References

Chapter 6: Appendix

Section 1: Molecular Cloning

Section 2: Fluorescent In Situ Hybridization Trouble Shooting

Section 3: Helpful Diagrams

Section 4: Further Explanation

Chapter 1: Background

Section 1: Importance of MicroRNA and Mammalian Skin Models

As more information about microRNAs is uncovered, their role in cellular processes becomes more significant. There are 222 identified microRNA in humans but it is estimated that there are at least 800 total human microRNAs (Bentwich et al., 2005). MicroRNAs play key roles in the regulation of many diverse physiological events including: stem cell differentiation, haematopoiesis, insulin secretion, cholesterol metabolism, and immune responses (Williams, 2008). The involvement of microRNAs in cancer is also an expanding field of research. MicroRNA expression levels can be used as a diagnostic tool for cancer patients as an aid in determining their prognosis (Lee and Dutta, 2009). MicroRNAs are known to regulate stem cell differentiation in mammalian skin. They are involved in embryonic development, hair follicle morphogenesis, and the regulation of bulge stem cells. In order to understand the development of hair follicles and regulation of skin stem cells, it is vital to understand microRNA's role in the skin cells.

The skin is a barrier between the external environment and the body and as a result is exposed to many toxins and different environments. In order to protect the body from harmful exposures and injury, the skin must have the ability to regenerate quickly. The skin is an ideal organ to study stem cell differentiation because of its regenerative properties and the ease of tissue acquisition.

Section 2: Importance of Stem Cell Regulation

Stem cells are undifferentiated cells with the capability to self-renew and differentiate to become different cell types. There are four categories of stem cells: totipotent, pluripotent,

multipotent, and unipotent. Each type of stem cell has the capability of producing other cells; the distinction between each type is the amount and variety of cells they can renew. Totipotent cells are able to form all cells of an embryo including the somatic and germline cells of the zygote, as well as the surrounding placenta. Totipotent cells can differentiate into pluripotent cells; these cells are able to differentiate into all three germ layers of an embryo: endoderm, mesoderm, and ectoderm. Once tissues become more specialized, multipotent cells become the stem cell population. Multipotent stem cells, the most abundant stem cells in adults, are responsible for the differentiation and creation of cell lineages. These stem cells have the ability to re-new and regenerate multiple cell lineages in a given system. For example, the skin has a very high turnover rate and thus needs to repopulate the epithelial cells, in addition to maintaining other cell types such as the sebaceous gland cells. If only one type of cell needs to be regenerated, unipotent stem cells can repopulate those specific types of cells.

Stem cells are fascinating because their ability to regenerate tissue and organs holds promise in the treatment of diseases. Although stem cells are unique for their ability to regenerate, stem cells also play an important role in forging the front of personalized medicine and drug screening. Stem cells have interesting regulation mechanisms that can help scientists understand cellular regulation, disease pathways, and tissue regeneration. The regulatory mechanisms and manipulation of stem cells can be applied in human biology and medicine, particularly cancer and the regeneration of damaged tissues. Knowing what turns a stem cell "on and off" will lead to greater insight as to how stem cells differentiate or stay in an undifferentiated state.

There are many hypotheses describing the regulation of stem cells. One hypothesis is that the environment surrounding the stem cell population produces signals that keep the cells in an

undifferentiated state until they leave that environment. This environment is often referred to as a stem cell niche. Another current hypothesis suggests that stem cells are inherently different and already have a cell autonomous fate. In this model differentiation signals come from within the cell, possibly signaled from an event outside the cell or even an adjacent stem cell (notch/delta signaling), that lead to that stem cell's differentiation.

In reality, the regulation of stem cells is a dynamic process that includes several different regulatory strategies. Over the past decade microRNAs have emerged as a central regulatory mechanism in the gene expression of many different cell types and show promise in broadening our understanding of how stem cells become committed to a specific cell lineage.

Section 3: MicroRNA Biogenesis and Function

The Central Dogma of Biology describes the flow of information from DNA to RNA to protein. Deoxyribonucleic acid (DNA) is transcribed into ribonucleic acid (RNA), which is then translated into protein. Figure 1.1 illustrates how microRNA affects the central dogma.

Figure 1.1

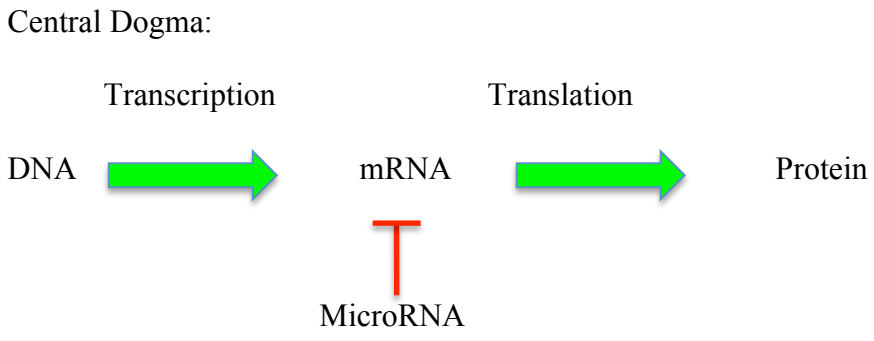

DNA is the template for messenger RNA (mRNA), which is transcribed within the nucleus. Once the RNA is transcribed, it is processed and transported from the nucleus to the cytoplasm. The messenger RNA is translated into protein by ribosomes that are located in the cytoplasm and on the endoplasmic reticulum.

MicroRNAs are regulatory molecules that function by inhibiting the translation of mRNA transcripts. They can act by targeting the mRNA for degradation or by inhibiting initiation factors needed for the start of translation. Thus microRNAs are able to regulate the number of transcripts that are available for translation and ultimately the protein concentration in cells. This protein regulation can affect a variety of physiological events.

MicroRNAs are non-coding RNAs that are 20-23 nucleotide (nt) sequences. Since they are non-coding transcripts, they are often found in introns and intergenic regions of DNA (Bostjancic and Glavac, 2008). Intergenic regions were once thought to be "junk" DNA because they did not produce transcripts for coding proteins. It was also thought that non-coding regions of DNA served no functional purpose in cells. These views on the non-coding regions of DNA are no longer thought to be valid. It is widely accepted that previously overlooked DNA regions (including those that encode microRNAs) actually serve a vital role in regulating transcript and protein levels.

MicroRNAs are transcribed from intergenic and intron regions by RNA Polymerase II (RNA Pol II) (Figure 1.2). The resulting transcript is a primary microRNA, pri-miRNA.

The pri-miRNA forms a hairpin structure with two stands of 30 nucleotides (nt) base paired to each other with a loop on the top. It is processed A microprocessor complex composed of Drosha and DiGeorge syndrome Critical Region Gene 8 (DGCR8) catalyzes this cleavage event. Together Drosha/DGCR8 are responsible for the cleavage the pri-miRNA to precursor microRNA or pre-miRNA.

Once the pre-miRNA is created in the nucleus, it is exported to the cytoplasm via exportin5, a member of the nuclear transport receptor family, previously known to transport tRNA to the cytoplasm (Kim et al., 2009). After the pre-miRNA has been successfully transported out of the nucleus, full maturation can take place.

In the cytoplasm, Dicer, a highly conserved enzyme in eukaryotes, binds and cuts the pre-miRNA at the top of the hairpin loop resulting in a duplex of RNA about 22 nt in length (Kim et al., 2009). Argonaute (Ago) proteins then bind to the newly cut RNA; however, they only bind one strand, which becomes the guide strand. The guide strand will be the mature microRNA used to target endogenous mRNAs. The other 22 nt strand, known as the passenger stand, will be degraded by specific mechanisms that have not been fully elucidated (Kim et al., 2009).

Once Ago has made its selection as to which strand will be utilized as the mature miRNA, Dicer binds to the Ago-RNA segment, thus forming an RNA-Induced Silencing Complex (RISC). Once the RISC complex is fully assembled, the miRNA is able to find and bind to its target mRNA, thereby preventing the mRNA from being translated. If the miRNA targeting is potent and efficient, the change in gene expression can alter the fate of the cell.

Figure 1.2 (Kim et al., 2009)

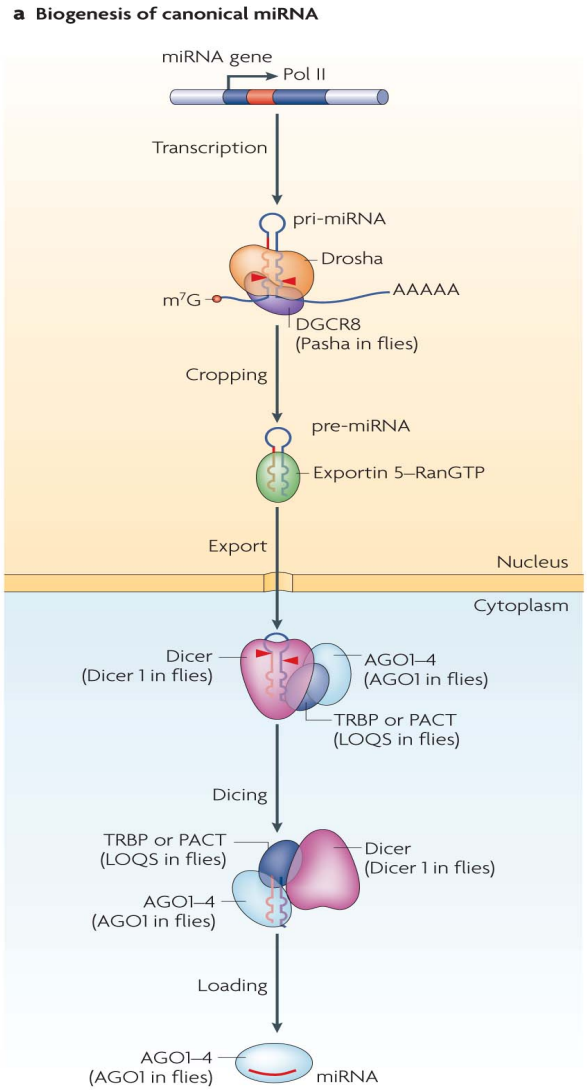

miRNA biogenesis pathway. a | Canonical microRNA (miRNA) genes are transcribed by RNA polymerase II (Pol II) to generate the primary transcripts (pri-miRNAs). The initiation step (cropping) is mediated by the Drosha–DiGeorge syndrome critical region gene 8 (DGCR8; Pasha in *Drosophila melanogaster* and *Caenorhabditis elegans*) complex (also known as the Microprocessor complex) that generates ~65 nucleotide (nt) pre-miRNAs. Pre-miRNA has a short stem plus a ~2-nt 3′ overhang, which is recognized by the nuclear export factor exportin 5 (EXP5). On export from the nucleus, the cytoplasmic RNase III Dicer catalyses the second processing (dicing) step to produce miRNA duplexes. Dicer, TRBP (TAR RNA-binding protein; also known as TARBP2) or PACT (also known as PRKRA), and Argonaute (AGO)1–4 (also known as EIF2C1–4) mediate the processing of pre-miRNA and the assembly of the RISC (RNA-induced silencing complex) in humans. One strand of the duplex remains on the Ago protein as the mature miRNA, whereas the other strand is degraded. Ago is thought to be associated with Dicer in the dicing step as well as in the RISC assembly step. In *D. melanogaster*, Dicer 1, Loquacious (LOQS; also known as R3D1) and AGO1 are responsible for the same process. In flies, most miRNAs are loaded onto AGO1, whereas miRNAs from highly base-paired precursors are sorted into AGO2. The figure shows the mammalian processing pathways with fly components in brackets.

When encapsulated within RISC, microRNAs function by targeting and silencing mRNA transcripts. A typical target region for miRNA is the 3' untranslated region (UTR) of the transcript. When mRNAs are transcribed, not all of the transcript will be translated into a protein. The regions that are not translated are thus referred to as UTR's. MicroRNAs are able to bind specifically to these regions to inhibit translation or promote RNA degradation. MicroRNAs also have the ability to target multiple mRNA transcripts, leading to the coordinated alteration of gene expression that can change the fate and function of cells.

If the microRNA binds perfectly to the mRNA target, the transcript will be degraded (Valencia-Sanchez et al., 2006). However, if the binding is imperfect, the mRNA transcript will be translationally repressed. RISC is able to inhibit initiation factors preventing translation from occurring (Valencia-Sanchez et al., 2006). Regardless of the accuracy of RNA binding, microRNAs will decrease gene expression by either degrading specific mRNA transcripts or inhibiting the translation of those target mRNAs. Further detail of mRNA degradation and translational inhibition can be found the Appendix, Section 4.

Section 4: Skin Cell Lineages

The skin serves as a barrier to protect the body from the outside environment. In order to maintain and re-populate the stratified epithelium, skin stem cells must have the ability to self-renew and differentiate into different layers of the skin. The skin has many layers of cells composed of both the interfollicluar epithelium (skin between hair follicles) and the hair follicle. Understanding how micro RNAs regulate the development of stem cells into these different cell types with specific functions will aid the research of stem cells in general. The first step in

determining how microRNAs function and regulate stem cell differentiation is determining in which epithelial lineage those microRNAs are expressed.

Skin cell lineages are determined in embryogenesis and more fully developed a few weeks after birth. The general morphology of hair follicles during embryogenesis is known, but their regulation by microRNA is undetermined. Figure 2 illustrates the developmental stages of hair follicles and the interfollicluar epidermis.

Figure 1.3. (Yi and Fuchs., 2010)

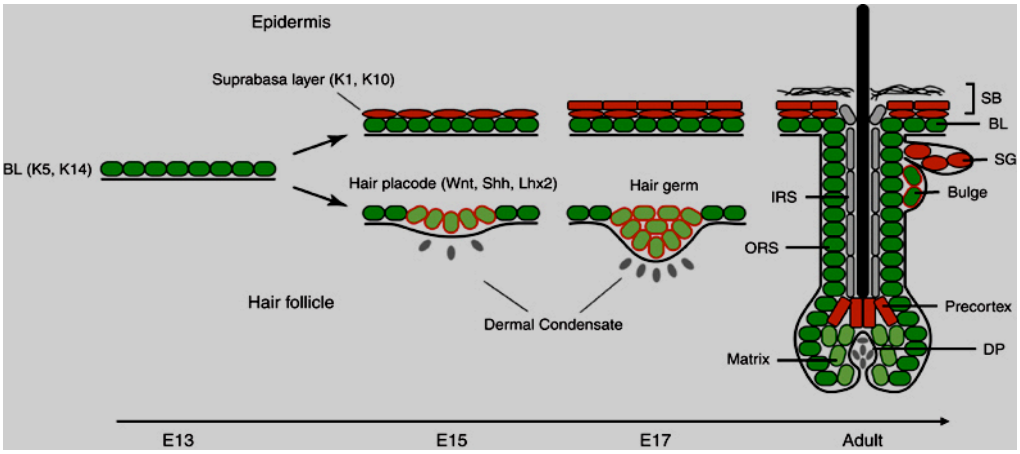

Figure 2 shows the development of the epidermis and hair follicle. Starting around Embryonic day 13 (E13), single layers of epithelial cells compose the basal layer (BL). This layer is marked by keratin 5 and 14. As a few days pass, the BL forms two different lineages: epidermis and hair follicle. The basal layer asymmetrically divides producing multiple layers of differentiated cells call the suprabasal layer (SB). Hair follicle development starts as the basal layer invaginates into the dermis. As the development progresses from the placode to mature hair follicle, several lineages of cells are created: bulge, outer root sheath (ORS), inner root sheath (IRS), pre-cortex fork, sebaceous gland (SG), and matrix cells.

During development, cells are assigned to different jobs. The jobs help carry out the functions of the skin and hair follicle. Terminally differentiated cells have been assigned a job

that they will carry out until they die. These cells do not replicate and therefore have no self-renewal capacity, but their job still needs to be done once these cells are gone. Undifferentiated cells are thus needed to regenerate the terminally differentiated cells. Figure 3 shows the cell lineages and their specified differentiated states.

Figure 1.4.

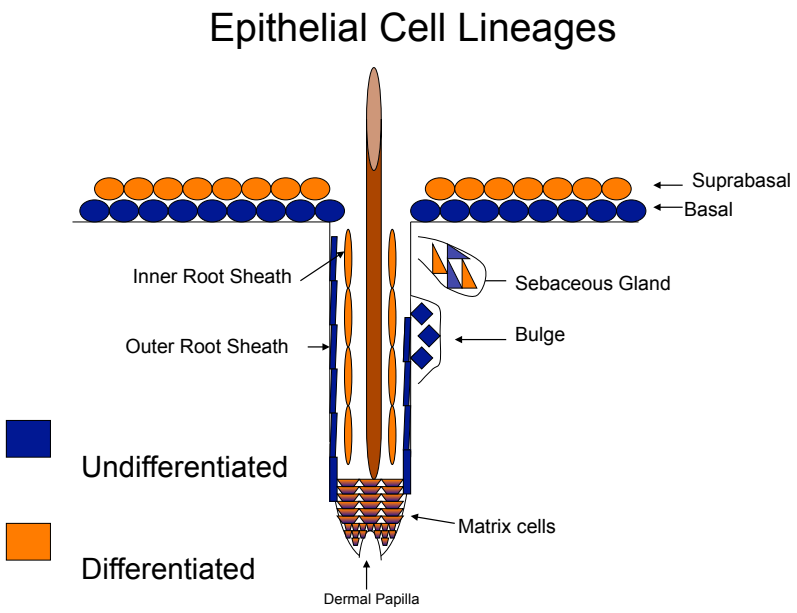

Figure 3 shows the different cell lineages and their relative state of differentiation. The blue cells are undifferentiated; they have more stem cell like properties. The bulge region and the basal layer are considered to be the stem cells responsible for re–constituting the interfollicluar epidermis and the hair follicle. The orange cells are more terminally differentiated cells. These lineages do not have the capacity to self-renew. The sebaceous gland is composed of both stem cells and terminally differentiated cells. The matrix cells are transit-amplifying cells. These cells are unique because they are rapidly dividing and differentiating simultaneously.

As cells in the epidermis travel closer to the environment and away from the basal layer they become more terminally differentiated. The differentiated cells in the epidermis are referred to as the suprabasal layer. The suprabasal layer includes the spinous and granular layers. The Stratum Corneum is composed of dead epithelial cells and therefore is not considered part of the suprabasal layer. Figure 1.5 clarifies the nomenclature.

Figure 1.5.

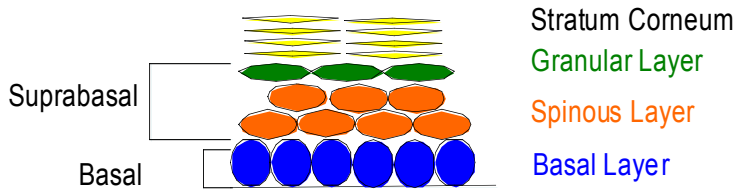

Illustration showing the orientation of the different cell layers in the epidermis.

Epithelial cells provide structure and protection for the body. Keratins are proteins found in epithelial cells that help provide structure and rigidity by creating scaffolds within the cells. Keratins are a family of proteins that are composed of many specific types of keratin. The different layers in the skin express different members of the keratin family. Basal cells express Keratin 5 and 14 (K5, K14), whereas the suprabasal layer cells expresses K1 and K10. These differences in keratin expression help researchers label and mark different cell types. As the cells differentiate and move toward the surface of the skin the keratins become longer and stronger eventually becoming fully keratinized in the stratum corneum layer.

Section 5: Hair Follicle Cycling

Mammals need to re-grow hair follicles frequently to compensate for wear and tear as well as seasonal changes. This consistent regeneration of hair follicles provides an excellent model for examining the regulation of stem cell differentiation.

Hair follicle cycles in most mammals consist of three main stages: anagen, catagen, and telogen. Hair growth takes place in anagen, while catagen is referred to as the disintegration of the hair follicle. Telogen is the rest period between catagen and anagen. Mice are a good model system for examining hair follicle regeneration because most mice undergo these three hair cycles. Several variables can affect the timing between stages in mice: genetic backgrounds, gender, nutrition, and environmental factors (Muller-Rover et al., 2001). Environmental factors include time of year, temperature, and light periods. Female mice are known to have longer telogen cycles than males.

Hair follicle development begins in murine embryogenesis and continues until the first catagen stage around postnatal day 16 (P16). At this point the hair follicle cycle starts and continues throughout the animal's life. Telogen soon follows catagen at P19, which is then followed by the first cycle of anagen, roughly from P28 until P42 (Figure 6). The depth of the follicle, position of Dermal Papilla (DP) cells, and the complexity of the follicle structure (Figure 7) characterize the stages of each cycle. For more details regarding hair follicle cycles see the Appendix, Section 4.

Figure 1.6 (Muller-Rover et al., 2001)

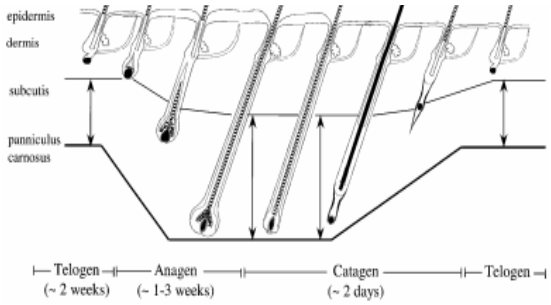

Figure 1.7 (Muller-Rover et al., 2001)

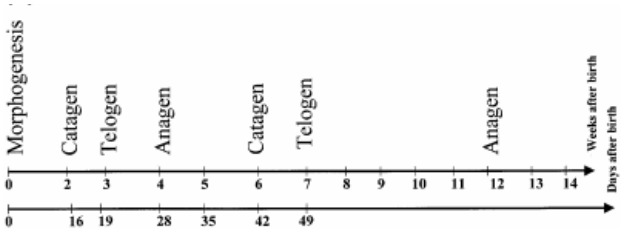

Figure 6 shows the progression of a full hair cycle starting from telogen through catagen.

Figure 7 shows the time frame for hair follicle cycling in increments of weeks.

Section 6: MicroRNAs in the Skin

MicroRNAs are found in mammalian skin tissue and are thought to play a role in hair follicle morphogenesis. It is believed that a discrete set of microRNAs are essential for the development of the hair follicles (Yi et al., 2006). This was determined by investigating hair follicle development in mice skin in the absence of microRNA. A knock-out mouse, in which the gene is completely removed from the animal, was created deleting Dicer. When this gene was absent, it was lethal for the mice suggesting that microRNAs are essential for normal development. In order to discern if microRNAs were essential to the development of the epidermis and hair follicle, a conditional knock-out mouse was made.

Conditional murine knock-out mice are animals where the gene of interest (Dicer) can be inactivated under certain conditions. These mice are used for studying the function of a gene when conventional knock-outs are lethal to the animal. For the purpose of discerning the role of microRNAs in hair follicle development, microRNAs were removed from skin cells, leaving all other cells functional. The resulting phenotypes of conditional Dicer knock-outs were mild in that the mice appeared dehydrated and small with minimal fat. However the life expectancy of

these mice was only four to six days after birth. Those phenotypes were not as crucial to understanding the role of microRNA as were the histological effects. A histological examination of the epithelial tissue of the conditional knock-out mice showed that even as the age of mice increased, visible "germ-like" cysts were still present in their skin cells. Usually after birth the epithelial cells have minimal cyst formations and more hair follicles. Hair germs were evaginated rather than invaginated. Hair follicles that were present before the deletion of Dicer showed arrested growth. Dicer deletion had obvious effects on hair follicles and their growth, but minimally affected the interfollicular epidermis (the areas surrounding hair follicles) (Yi et al., 2006). Yi determined that a subset of microRNAs must be differentially expressed in developing mice. Some of the most abundant microRNAs that were specific to skin were: miR-203, miR-205, miR-143, and miR-125b (Yi et al., 2006).

Section 7: Previous Knowledge and Published Data

If microRNAs can have differential expression patterns in the skin then they must have different functions. The expression pattern of miR-203 has been well characterized (Yi et al., 2008). However, the expression patterns and functions of the microRNAs miR-143, miR125b, and miR-205 in the skin have not been determined. The spatial and temporal expression of these microRNAs needs to be characterized in order to ascertain their function and role in hair follicle morphogenesis and stem cell regulation. It is helpful to look at the functions of microRNAs in other tissues because those functions might parallel that in the skin.

A. MiR-203:

MiR-203 is highly expressed in the suprabasal skin layer once differentiation begins in embryos 15.5 days after conception (Yi et al., 2008). Figure 7 shows the abundant expression of miR-203 specifically in the suprabasal layer in embryonic skin and in postnatal skin.

Figure 1.8

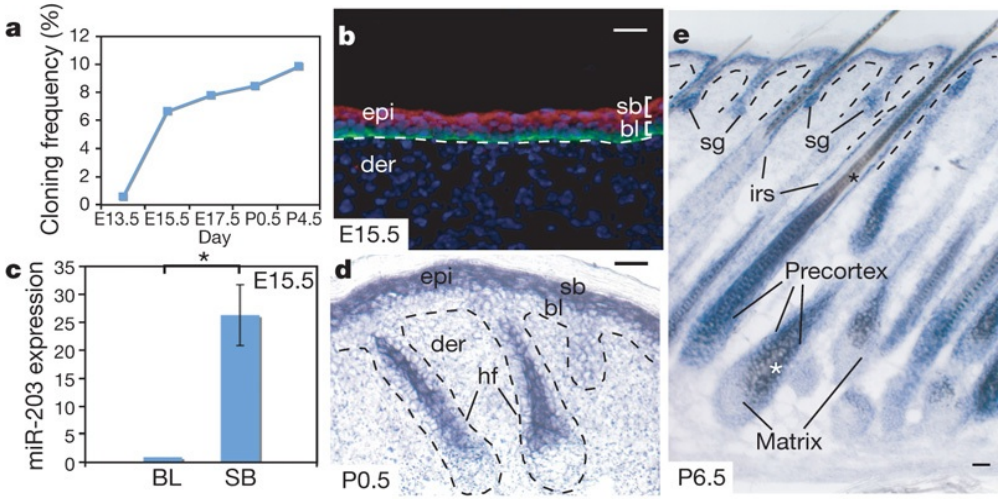

Temporal induction of miR-203 as measured by cloning frequency. **b, d**, **e**, *In situ* hybridization reveals restriction of miR-203 to suprabasal, differentiating layers of skin. sb, suprabasal; bl, basal layer; epi, epidermis; der, dermis; sg, sebaceous gland; irs, inner root sheath; hf, hair follicle. Asterisks in **e** represent brown melanin pigment that is not a hybridization signal. In **b**, anti-4-integrin co-labelling is in green and miR-203 *in situ* pseudocoloured signal is in red. **c**, qRT–PCR of FACS-purified cells from E15.5 epidermis reveals 25-fold more miR-203 in suprabasal (SB) versus basal layer (BL) cells (*$P < 0.002$). Error bars (s.d.) are derived from three experiments with basal layer level set as 1. Scale bars are 30 m (Yi et al., 2008)

Interestingly, Yi and colleagues discovered that one of miR-203's targets is P-63. P-63 is a protein that can drive cell differentiation and is important in stem cell maintenance, especially

in stratified epithelial tissues (Yi et al., 2008). MiR-203 is abundantly expressed in the skin and to date is not known to have important functions in other tissues.

B. MiR-143

MiR-143's expression is uncharacterized in the skin. However, in other research, miR-143 is expressed in tissues associated with smooth muscle (Cordes et al., 2009). Smooth muscle is located in vessels (blood and lymph) and tract systems including: gastrointestinal, reproductive, and respiratory. MiR-143 is as an important player in the maintenance of smooth muscle tissue and vascular homeostasis (Elia et al., 2009). MiR-143 is down regulated in human tissues that have aortic aneurysms (Elia et al., 2009). Thus, it is believed that a loss of miR-143 contributes to structural modifications of the aorta because there is incomplete differentiation of vascular smooth muscle cells (Elia et al., 2009).

MiR-143 is also implicated to have a functional role in prostate cancer (Clape et al., 2009). This micro RNA is thought to act as a tumor suppressor by inhibiting the expression of an oncogene. Human prostate cancer samples show down-regulation of miR-143 (Clape et al., 2009).

Adipose tissue is also affected by miR-143's presence. MiR-143 is positively correlated with adipose differentiation (Takanabe et al., 2008) indicating that this microRNA plays a similar role in fat cells as it does in smooth muscle cells, it promotes differentiation. When mice were fed a high fat diet, up-regulation of miR-143 was detected in the mesenteric fat (Takanabe et al., 2008). This data suggests a correlation between the expression of miR-143 and obesity.

To date, there are no reports of miR -143 expression in mouse skin cells, during embryonic, neonatal, or postnatal skin development. Microarray data from the Yi and colleagues

suggests miR-143 is expressed in matrix cells. However, this data needs to be supported by *in situ* hybridization to show the relative abundance and localization of miR-143 expression.

c. MiR-125b

The microRNA miR-125b acts to repress stem cell differentiation in skin cells (Zhang et al., 2011). Zhang et al, found miR-125b to be expressed in the upper outer root sheath, bulge, and basal cells. All of these cell types are undifferentiated cells that need to be triggered to differentiate. MiR-125b helps keep these cells in their undifferentiated state.

Figure 1.9 (Zhang et al., 2011)

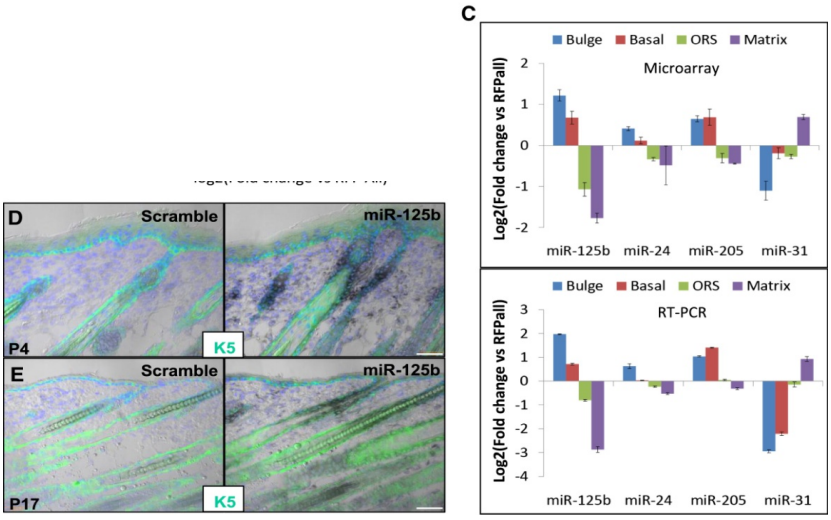

(C) miRNA-microarray results and RT-PCR verification of expression patterns of the miRs indicated. P6 was used as the reference gene in RT-PCR. Error bars represent standard error. (D and E) miR-125b in situ hybridizations of WT P4 and P17 back skins. In situ signals (black) were developed by BM purple substrate: K5 (green) in ORS and basal IFE. Scale bars represent 50 μm.

My results studying the expression of this microRNA were found before this publication. At the time of my studies, miR125b was a novel microRNA in the skin and other tissues.

D. MiR-205

MiR-205 is highly expressed in the skin, as shown by Yi and colleagues, but this microRNA has recently been found to play important roles in other tissues and cancer (Yi et al., 2006). It has also been suggested that miR-205 functions in progenitor cell populations.

MiR-205 was found to be present in a population of stem cells isolated from the mammary gland (Greene et al.,2010). These researchers found that miR-205 inhibited PTEN, a known tumor suppressor (Greene et al.,2010). The inhibition of a PTEN suggests that miR-205 encourages the cells to grow and divide, which are characteristic of stem cell populations. Mir-205 is expressed in other cells including neuronal precursor cells (Dogini et al., 2008) including those involved in olfactory neurogenesis (Choi et al., 2008).

Mir-205 is highly abundant in skin cells and functions in other tissues to promote stem cell characteristics suggesting that it may also play a role in skin stem cells. In order to explore this idea, the localization and transcriptional regulation of miR-205 needs to be determined in both embryonic and adult skin cells.

Section 8: Experimental Plan

MicroRNAs play different but vital roles in the progression of stem cells to terminally differentiated cells in the skin. I hypothesize that the microRNAs miR-203, miR-143, miR-125b, and miR-205 will be expressed in dissimilar skin and hair follicle cell lineages as a function of their differential role in the stem cells process.

One method to determine the expression pattern of microRNA is by *in situ* hybridization. This method allows researchers to characterize the location and relative abundance of microRNAs in cross-sections of tissue. Using this method I will compare the expression of the microRNAs miR-143, miR-125b, and miR-205 to the microRNA miR-203 (as a positive control)

in both embryonic and adult skin samples. I will also explore the relative expression patterns for miR-143 and miR-125b in postnatal mice from days four and six (P4 and P6). I will characterize the expression of miR-143 and miR-205 in embryonic tissue. The transcriptional regulation of miR-205 may be key to understanding the differentiation of skin stem cells. MiR-205 is the second most abundant microRNA in the skin, and is potentially a regulating factor in skin stem cells.

Once the expression pattern for miR-205 is elucidated, I will examine how it is regulated in the specific cells in which it is expressed. I will investigate potential promoter regions that activate the transcription of miR-205 using luciferase assays. I will assay several different DNA regions that are hypothesized to drive the expression of miR-205.

Chapter 2: Methods and Materials

Section 1: In Situ Hybridization

In situ hybridization (ISH) is a technique that is used to label DNA and RNA in tissues. ISH can be used to determine the spatial and temporal expression patterns of microRNA expression. In my experiments, I will use this technique to show the localization and relative abundance of microRNA in skin sections. There are two different methods of ISH: Nitro-blue-tetrazolium with 5-bromo4-choloro-3 indolyphosphate (NBT/BCIP) and Fluorescent In Situ Hybridization (FISH). Below is an illustration highlighting the important steps in both *in situ* hybridization methods. For a more detailed explanation of this technique please refer to the appendix (Section 2).

Figure 2.1

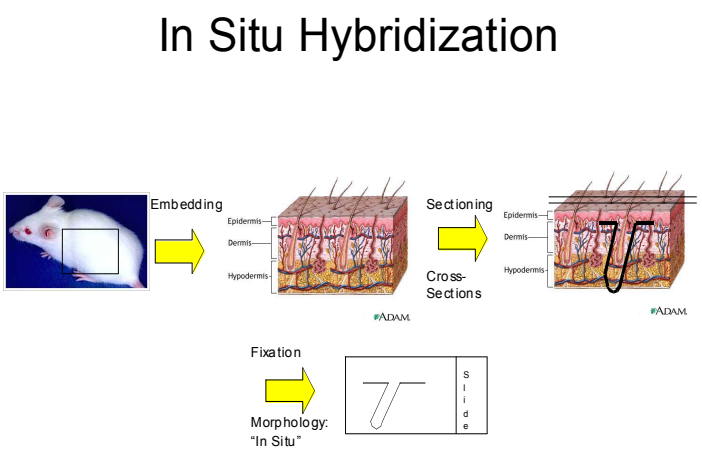

In order to study the skin, samples are taken from the backs of mice. They are embedded into OCT and frozen. Once they are frozen, sections are made by cutting the block of frozen tissue in a cross-sectional manner. Cut sections are transferred onto glass microscope slides and fixed with 4% paraformaldehyde (PFA). This cross-links proteins to each other preserving the tissue.

Figure 2.2

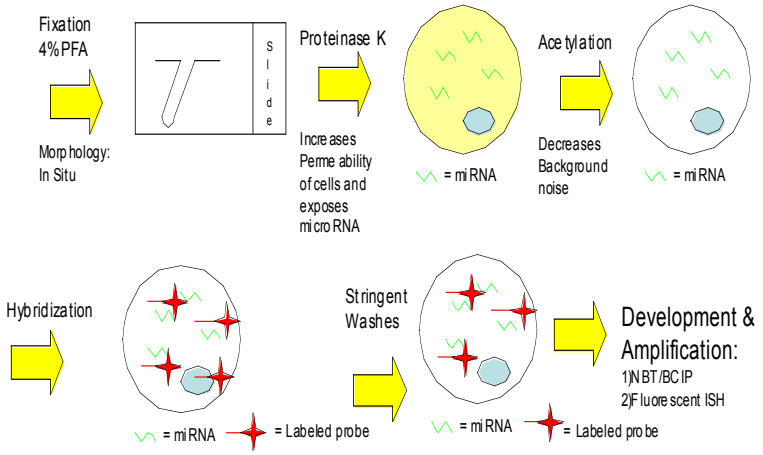

After the sections have been fixed, Proteinase K is added. Proteinase K degrades proteins in the cells to expose microRNA and permeabilizes the cells for the probe to have easier entry. Acetylation of the tissue decreases the background noise from non-specific hybridization. Locked nucleic acid (LNA) probes (from Exiqon) labeled

with Digoxigenin (DIG) are used as probes to hybridize to the microRNAs. The probes are labeled with Digoxigenin, which is recognized by the antibodies in this assay. This is ideal for ISH detection.

The synthetic nucleotide sequences of these probes have altered structural confirmations that increase the stability of dsRNA, which is critical for microRNA hybridization. The LNA probes help stabilize the microRNA/probe duplex preserving and potentially amplifying genuine signals. It is important to stabilize these duplexes when exploring microRNA expression patterns because some microRNAs are not as abundant and any degradation or instability in the probe could alter the hybridization signal.

After the probes have been hybridized to the microRNA, either NBT/BCIP or Fluorescent ISH methods are used to amplify the microRNA signal.

A. NBT/BCIP produces a "black and white picture". For NBT/BCIP, an alkaline phosphatase (AP) enzyme is attached to the antibody regcognizing the DIG label on the probe (Anti-DIG). This enzyme converts the substrate into a dark precipitate. The substrates for this reaction are: nitro-blue tetrazolium (NBT) and 5-bromo-4-chloro-3'-indolyphosphate (BCIP). After several hours, the dark precipitate is localized to the target microRNA. Figure 2.2 shows the recognition and enzymatic reaction leading to the precipitation product.

Figure 2.3

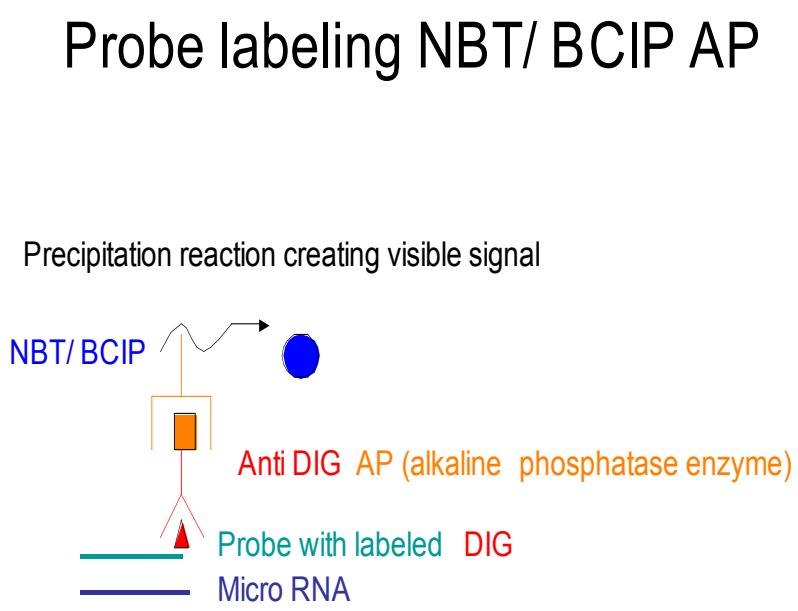

Once the probe is hybridized to the microRNA, an antibody conjugated with alkaline phosphatase (AP) recognizes and binds to the DIG label. When the substrates are added, AP will catalyze the reaction and leave a dark precipitate where the microRNA is located.

B. Fluorescent In Situ Hybridization (FISH) is similar to NBT/BCIP. FISH differs in method because it uses an antibody that recognizes the DIG label on the probe but the antibody is conjugated with horse-radish peroxidase (POD) enzyme rather than alkaline phosphatase. The substrate is Tryamide, which is converted into a fluoroform. (Specific details of this reaction can be found in the Appendix Section 5).

Amplification of the fluorescent label only takes several minutes as opposed to several hours with NBT/BCIP. After amplification, the sections can be co-stained and visualized using different light channels. In these experiments Beta 4 integrin is commonly used to label the lining of the basal layer and the nucleus of the cells is dyed with Hoechest, a fluorescent dye that

is incorporated into the DNA. These co-stains are important because they provide context and the contrast necessary to detect the fluorescently labeled microRNA on a sub-cellular basis.

Figure 2.4

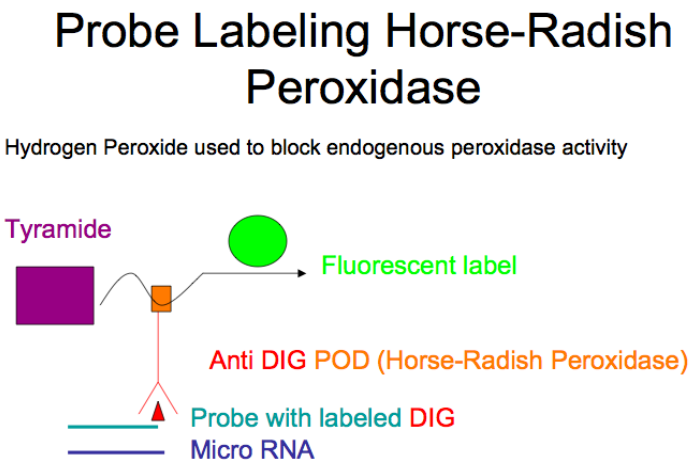

After the DIG labeled probe has been hybridized to the microRNA, anti-DIG POD is added to the prepared tissue. This antibody which is conjugated to a peroxidase enzyme recognizes the DIG label . Before the Tyramide substrate is added, hydrogen peroxide is used to inactivate endogenous peroxidase activity. Amplification usually takes between 5-15 min.

Confocal microscopy was used to detect the FISH labeled micro RNAs in the tissue samples. Confocal microscopes can produce a three-dimensional image since they have three axes: X, Y, and Z, (Other microscopes have an X and Y axis which gives a two-dimensional picture of a slide). Confocal microscopy produces extremely high-resolution pictures showing sub-cellular localization of microRNA. (See the Appendix, Section 5 for a visual representation of confocal imaging).

In situ hybridizations were performed with both NBT/BCIP and FISH on embryonic, neonatal, and adult murine skin. Sections varied in thickness but ranged between 10-14μm (See Appendix Section 5 for a more detailed description of embedding and sectioning).

Section 2: Real Time Quantitative Polymerase Chain Reaction (RT-qPCR)

Real Time Quantitative Polymerase Chain Reaction **(**RT-qPCR) is a way to quantify the relative amount of a specific amplified DNA sequence. This method was used to identify and quantify various microRNA levels. RT-qPCR is based on the polymerase chain reaction (PCR) technique. PCR is a technique that amplifies specific sequences of DNA. Primers are made that flank both the 5' and 3' ends of the DNA sequence of interest and direct the DNA polymerase to synthesize new complimentary strands of that target DNA sequence. This synthesis reaction is repeated in a number of cycles that allows the target DNA to be amplified exponentially.

Quantitative PCR uses the same technique as PCR, however the amount of the amplified DNA is measured by quantifying fluorescence readings. Fluorescent dyes are added to the reaction and get incorporated into the newly synthesized double stranded DNA. As each cycle of amplification is completed, the fluorescent intensity of that DNA is measured and recorded. These data can be used to detect DNA to compare relative DNA abundance to other samples.

Section 3: Real Time Quantitative PCR to determine microRNA expression levels

In order to quantify and explore microRNA in other tissues, the RNA was extracted from those tissues, complementary DNA (cDNA) was made from that RNA using reverse transcriptase and the resulting DNA was then used as a template in RT-qPCR reactions.
The microRNA was initially isolated from tissue by homogenizing the tissue in Trizol. Trizol is a reagent that extracts DNA, RNA, and protein (Chomczynski and Sacchi, 2006). RNA was then isolated using isopropyl alcohol precipitation.

Reverse transcription of the RNA precipitate was completed using Qiagen's miRscript RT kit (one hour incubation at 37degress Celsius, followed by a 5 minute incubation at 95 degrees Celsius, and stored at 4 degrees Celsius).

The cDNA were then used as templates in RT-qPCR to quantify microRNAs. The fluorescent intensity of these cDNAs were compared to endogenous microRNA cDNAs that are known to be expressed in all cells: Sno25 and Let7a.

BioRad iQ SYBR Green supermix was used to fluorescently label the microRNA cDNA under the following RT-qPCR conditions

95°C 15 min

95°C 15 sec

55° C 30 sec

72° C 30 sec

39 cycles

4° C ∞

Section 4: Luciferase Assay

A luciferase assay can be used to determine if a region of DNA has promoter activity. The luciferase gene (responsible for luminescence in fireflies) has been isolated and cloned into a vector called pGL3. The pGL3 vector also contains essential plasmid elements: an origin of replication, a multiple cloning site, the ampicillin resistance gene (beta lactamase), and the luciferase gene (Figure 2.3). There are three types of pGL3 constructs that were used in these experiments: pGL3 Basic, pGL3 Control, and three pGL3 constructs A, B, and C.

PGL3 Basic serves as a negative control for the luciferase assay. This plasmid has all of the necessary elements of the vector (an origin of replication, a multiple cloning site, the

ampicillin resistance gene (beta lactamase), and the luciferase gene) but lacks the promoter region for the luciferase gene. With no promoter region, the luciferase enzyme cannot be transcribed or translated. The pGL3 plasmid contains the identical elements of pGL3 Basic, but also has the SV40 promoter positioned in front of the luciferase gene. The SV40 promoter is derived from the SV40 virus and is transcriptionally active in eukaryotic cells. The experimental plasmid constructs pGL3 A, B and C are made by inserting the DNA of interest into the multiple cloning site of the pGL3 Basic vector in front of the luciferase gene. If any of these DNA inserts have promoter activity they will drive the expression of the luciferase gene. These constructs are referred to as A, B, and C to indicate the three different DNAs that were cloned into this vector.

Figure 2.5

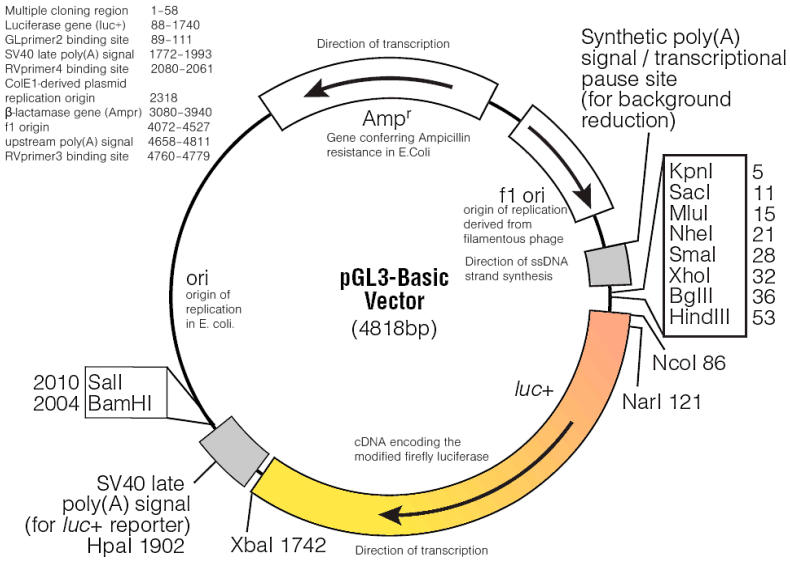

The pGL3 Basic vector that will be used to clone DNA sequences of interest is diagrammed above. The multiple cloning site is shaded grey and is positioned in front of the luciferase gene (shaded orange/yellow). The beta lactamase gene conferring ampicillin resistance is opposite the luciferase gene

The pGL3 constructs will be transfected into wild type keratinocyte cells and luciferase activity will be measured. The protein product produced from these constructs is a recombinant

luciferase enzyme, which catalyzes beetle luciferin to oxyluciferin (Promega Technical Manual) (Details of this reaction can be found in the Appendix, Section 5). Luciferase activity will be specifically assayed by lysing the cells 48 hours after transfection, adding beetle luciferin to the lysed cells and measuring the production of oxyluciferein by a luminometer.

Promega's Dual Luciferase Reporter Assay System utilizes both the pGL3 firefly luciferase vector and a renilla luciferase plasmid. These two luciferase enzymes, recombinant firefly luciferase and renilla luciferase, bind different substrates and produce different products (See the Appendix, Section 5). Both products can be detected by a luminometer. This dual luciferase assay, provides an internal transfection control. Essentially, if the ratio between recombinant firefly luciferase and renilla luciferase is detectably different, then that difference suggests the promoter activity from the pGL3 construct. Renilla Relative Fluorescent Units (RFU, detected by the luminometer) provide a standard fluorescent unit to compare the fluorescence of all of the pGL3 controls and constructs.

Renilla and pGL3 plasmids were co-transfected into wild types keratinocytes for 48 hours using MiRus TransIT LT1 transfection agent. MIGR effector plasmid was also used as a transfection control to determine transfection efficiency. This plasmid contains green fluorescent protein (GFP) under the control of a viral promoter. If the transfection was successful, the GFP gene would be transcribed and translated inside the cell and be easily detected

Section 5: Molecular Cloning

Three pGL3 constructs were made with using different potential promoter regions of miR-205. All constructs were made by:

A. Creating an insert (using a plasmid created for miR-205 knock-out, as a template);

B. Restriction enzyme digestion of the insert and vector with HindIII and Nhe1 to create complementary ends;

C. Ligating the insert into pGL3 Basic plasmid using NEB's Quick ligase (incubating at room temperature for 10-15min);

D. Transforming the plasmid into JM109 competent cells: 10min incubation on ice, 45sec heat shock at 42 degrees C, 2 min incubation on ice. The cells were then plated on ampicillin positive plates for 12-16 hours;

E. Selecting positive colonies on ampicillin agar plates;

F. Verification of the constructs was done by isolating plasmid DNA from the transformed cells, and restriction digest analysis of those plasmids to confirm proper length and orientation;

G. All final constructs pGL3 A, B, and C were sequenced to verify the sequence, length and orientation of the insert.

Figure 2.6: Demonstrates the importance of proper orientation of the insert into pGL3 Basic

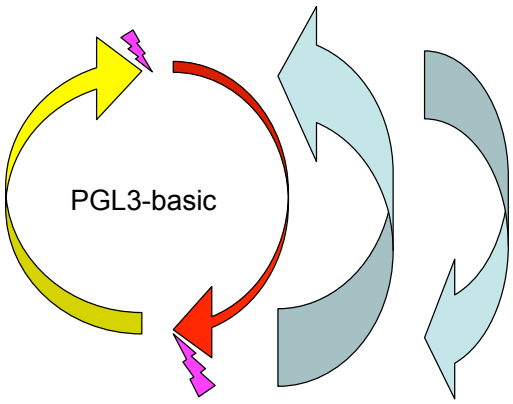

As shown in Figure 2.4, if the promoter DNA was ligated in pGL3-Basic in the counterclockwise direction, the luciferase gene will not be transcribed and no luminescence will be detected. The pink lightning bolts indicate the restriction enzyme (R.E.) sites where the insert was ligated into the plasmid. The red arrow

indicates the predicted promoter region. The luciferase gene is highlighted in yellow showing the direction of transcription (clockwise).

In pGL3 205 A, the insert was created by enzyme digestion of the target plasmid. The target plasmid had HindIII sites flanking 8.302 Kilo basepairs (KB) that was the target region. This region was isolated after digestion and was then ligated with both ends of the insert complementary to the HindIII site in the vector. PCR screening was necessary to determine proper orientation. Primers were created to

In the second construct, pGL3 205B the insert was 3.5KB. PCR reaction was used to generate the DNA insert utilizing primers that contained the appropriate restriction enzyme sites. For example the 5' primer used for PCR had an Nhe1 site, whereas the 3' end of the insert was amplified by a primer that contained a HindIII site. The insert was cut with Nhe I and Hind III and then ligated into the multiple cloning site of pGL3 Basic (which had been cut with NheI and Hind III).

Due to the GC rich sequence 10% DMSO was needed in the PCR reaction to obtain a product. Standard PCR conditions were used along with New England Biolab's (NEB) phusion enzyme and HF buffer.

The PCR conditions used to generated the DNA inserts were as follows:

98°C 15 min

98°C 15 sec

56° C 30 sec

72° C 30 sec

35 cycles

4° C ∞

The method used to create the insert for construct pGL3 205C was identical to that of construct pGL3 205B except that a different 3' primer was used to create a shorter DNA insert (2.7KB).

Chapter 3 Results:

Section1: MiR-203 Expression Pattern

MiR-203 is expressed in differentiated cell lineages including the suprabasal layer (SB), the sebaceous gland (SG), the inner root sheath (IRS), and the pre-cortex fork (PCF). NBT/BCIP *in situ* hybridization has confirmed these expression patterns, but further clarification using FISH is needed to distinguish the expression of this microRNA in the epidermis. These hybridization experiments also need to be done with a negative control so that artifacts of the *in situ* procedure could be ruled out and relative background noise will be visible.

Figure 3.1

Illustration of the observed miR-203 Expression

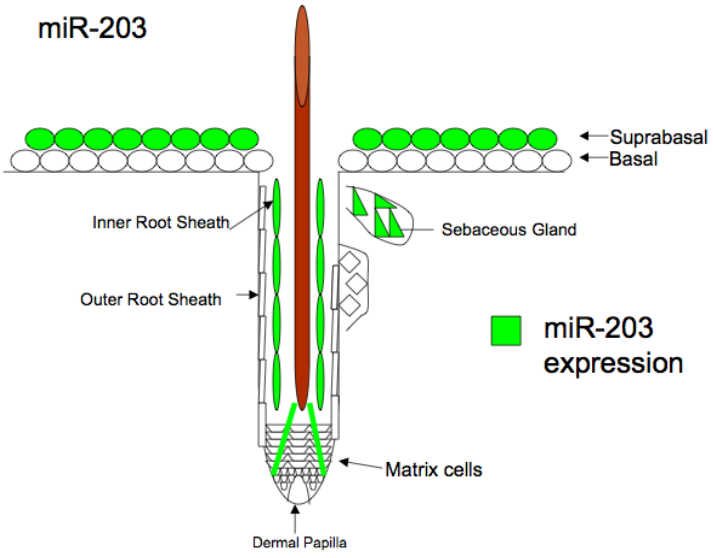

A. NBT/BCIP in situ hybridization

The different cell lineages were labeled as described in the Materials and Methods section.

Figure 3.2

MiR-203 NBT/BCIP

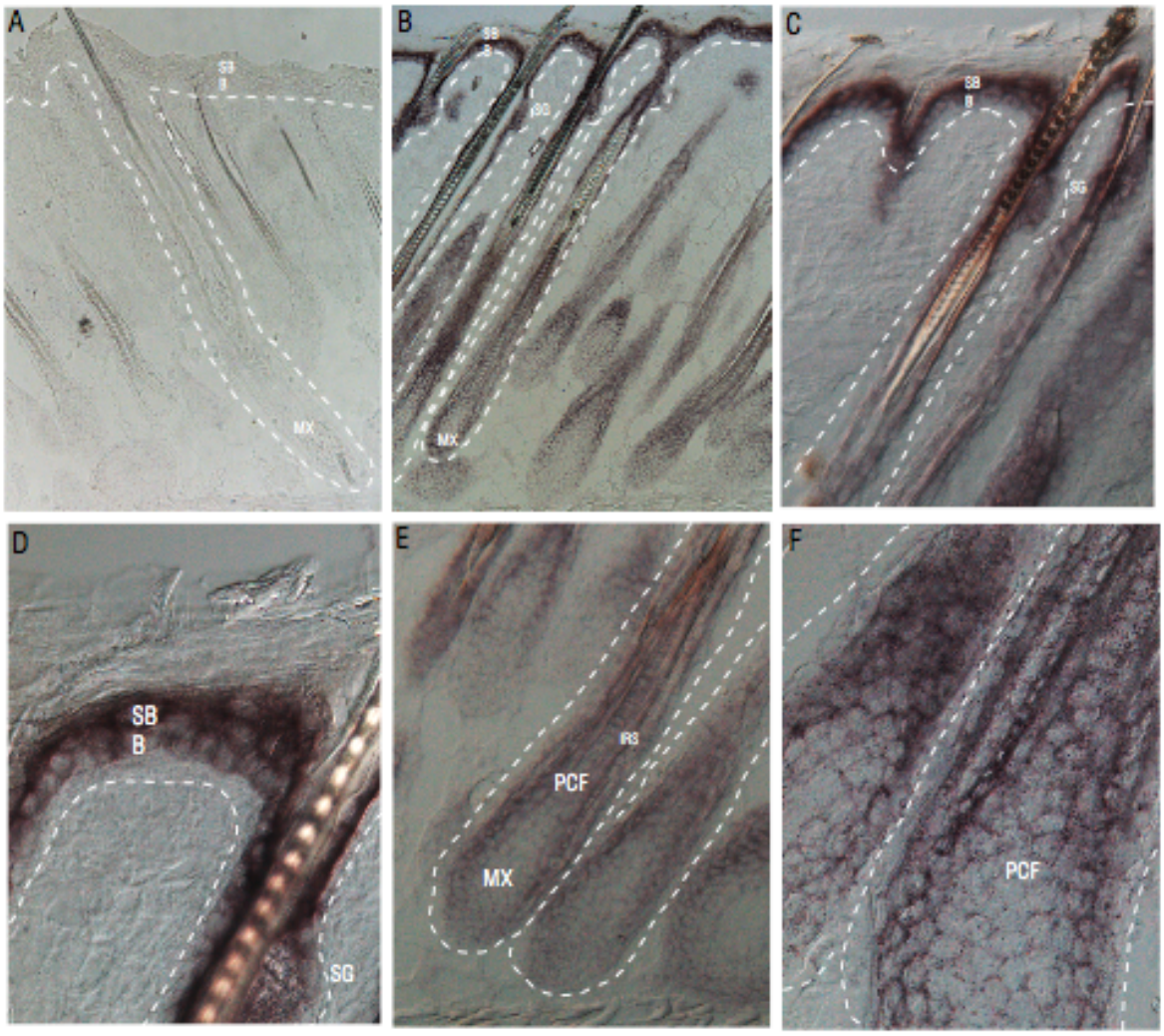

MiR-203 Expression in Postnatal day 6 (P6) mice: A) Negative control at 10x magnification lacking the probe B) Hybridization using miR-203 probe at 10x magnification, dark staining regions indicate strong miR-203 expression in the epidermis, specifically the suprabasal layer (SB). C) Hybridization using miR-203 probe 20x magnification the dark areas indicate strong expression of miR-

203 in the suprabasal layer. The signal in the basal layer needs to be clarified with FISH for further verification. This image also shows miR-203 expression in the sebaceous gland (SG). The inner root sheath is also visible. D) Hybridization using miR-203 at 63x magnification: This image shows the expression of miR-203 in the basal and suprabasal layer E) Hybridization using miR-203 probe at 20x magnification: miR-203 expression is visible in the inner root sheath, pre-cortex fork, and the matrix F)) hybridization using miR-203 probe at 63x magnification: miR-203.is clearly expressed in the PCF and stems from the inner root sheath.

B. Fluorescent in situ hybridization:

FISH was used to clarify the expression of miR-203 in the epidermis of postnatal day 6 (P6) mice. The FISH technique allows the investigator to visualize the sub-cellular localization of miR-203 (labeled with a green fluorescent tag) as well as other fluorescently tagged molecules including Beta-4 integrin (red) and the nucleus (blue). MiR-203 is preferentially expressed in the suprabasal layer (Figure 3 panel E). The negative control (Figure 3 Panel A) is back skin isolated from an miR-203 conditional knock out (DGCR8, see Materials and Methods). These mice lack one of the complexes used in microRNA biogenesis. No mature microRNA should be expressed in epidermis isolated from these mice.

Figure 3.3

MiR-203 Fluorescent *in situ* hybridization

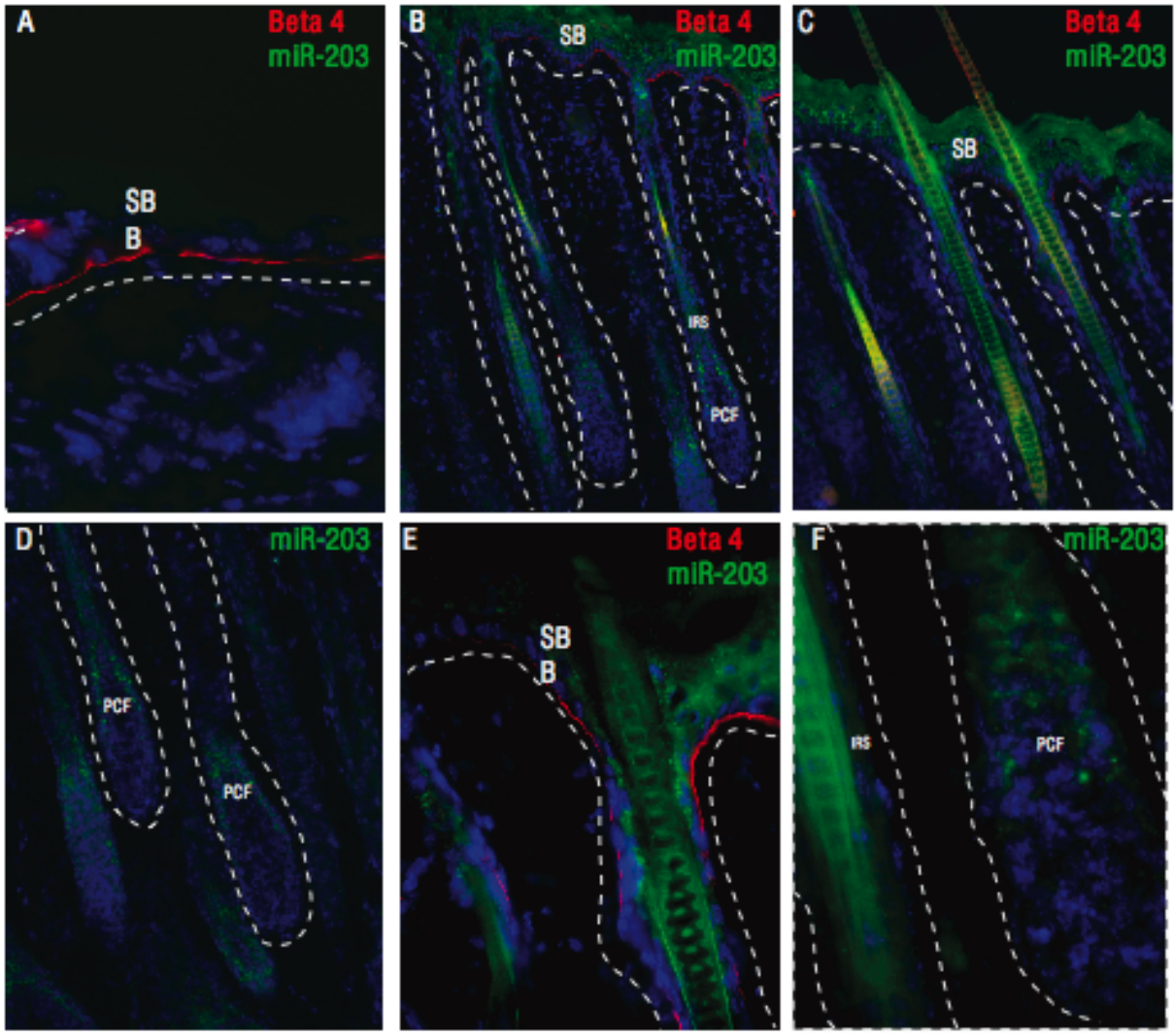

MiR-203 Expression in Postnatal day 6 (P6) mice: A) FISH results at 20X magnification using back skin isolated from DGCR8 knock out mouse. B) FISH results at 20X magnification indicating the general expression pattern of miR-203, beta 4-integrin expression in the suprabasal layer, inner root sheath, and the pre-cortex fork. C) FISH results at 20X magnification shows the expression of miR-203 in the suprabasal layer. The beta-4 integrin staining is weak but the basal layer is located above the white line in the image. D) FISH results at 20X magnification verifies the expression of miR-203 in the PCF. E) FISH results at 63X magnification indicating that miR-203 is specifically localized to the suprabasal

layer. The labeling of SB and B marks the distinction in expression between the two layers. F) FISH results at 63X magnification shows miR-203 expression is further verified in the PCF, and localized in the inner root sheath of the hair follicle adjacent to the labeled matrix. The inner root sheath is distinct because its cell shape is long and skinny, this image supports but does not confirm the expression of miR-203 in the inner root sheath.

Section 2: MiR-143 Expression Pattern

MiR-143 is expressed in matrix cells and minimally expressed in the epidermis, specifically the suprabasal layer (Figure 3.5). The images from the FISH experiment (Figure 3.6) support the observed expression of miR-143 in matrix cells, with minimal expression in suprabasal layer. The negative control was not hybridized to any probe and therefore shows background signal in Figure 3.5.

Figure 3.4

Illustration of observed miR-143 Expression

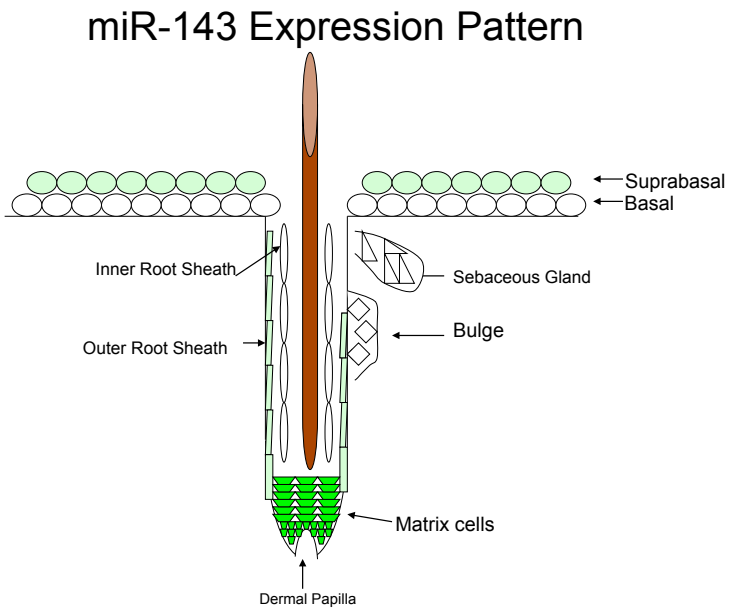

A. NBT/BCIP in situ hybridization

Figure 3.5

MiR-143 NBT/BCIP

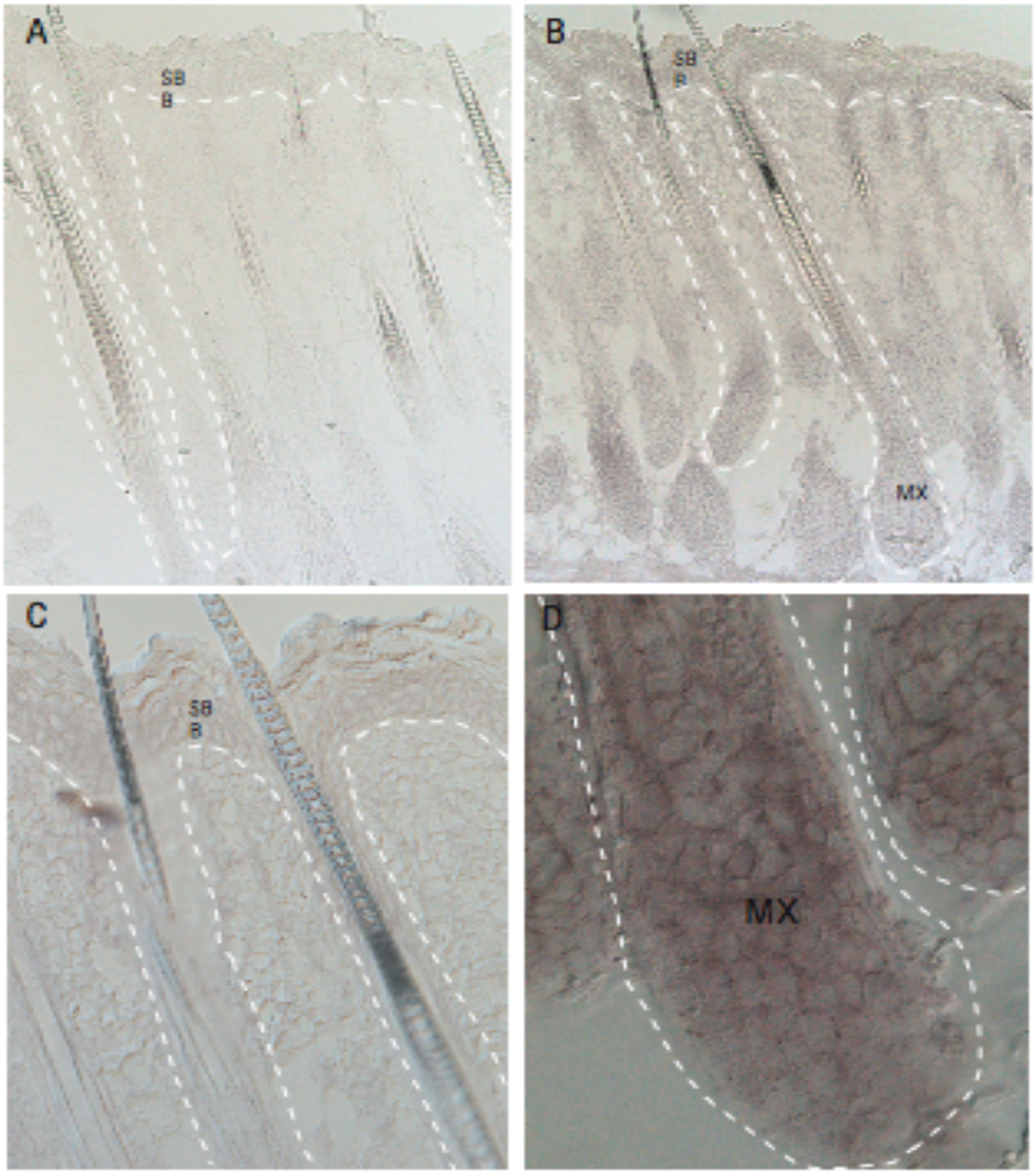

Note: These samples are slightly underdeveloped so the abundance of microRNA may not be reflected accurately by the signal strength. MiR-143 Expression in Postnatal day 6 (P6) mice: A) Negative control no probe was added to this slide. B) MiR-143 expression at 10x magnification: evident in the matrix and

slightly expressed in the epidermis C) Epidermis from back skin at 20x magnification: this image shows minimal miR-143 expression in the epidermis.. D) Matrix from back skin at 63x magnification demonstrating that miR-143's expression is uniform in the matrix.

B. Fluorescent in situ hybridization (FISH)

MiR-143 is expressed in the matrix of developing hair follicles. MiR-143 shown in green, nucleus is stained with Hoechst (blue). The hair shafts in these pictures have auto fluorescence. Non-specific signals can be seen in the bright hair shafts and the stratum corneum (SC) (a layer of dead epidermal cells). The negative control is a Dicer conditional knock out, with the probe added. This is another important molecule involved in microRNA biogenesis. No genuine expression is detected.

Figure 3.6.

MiR-143 Fluorescent *in situ* hybridization

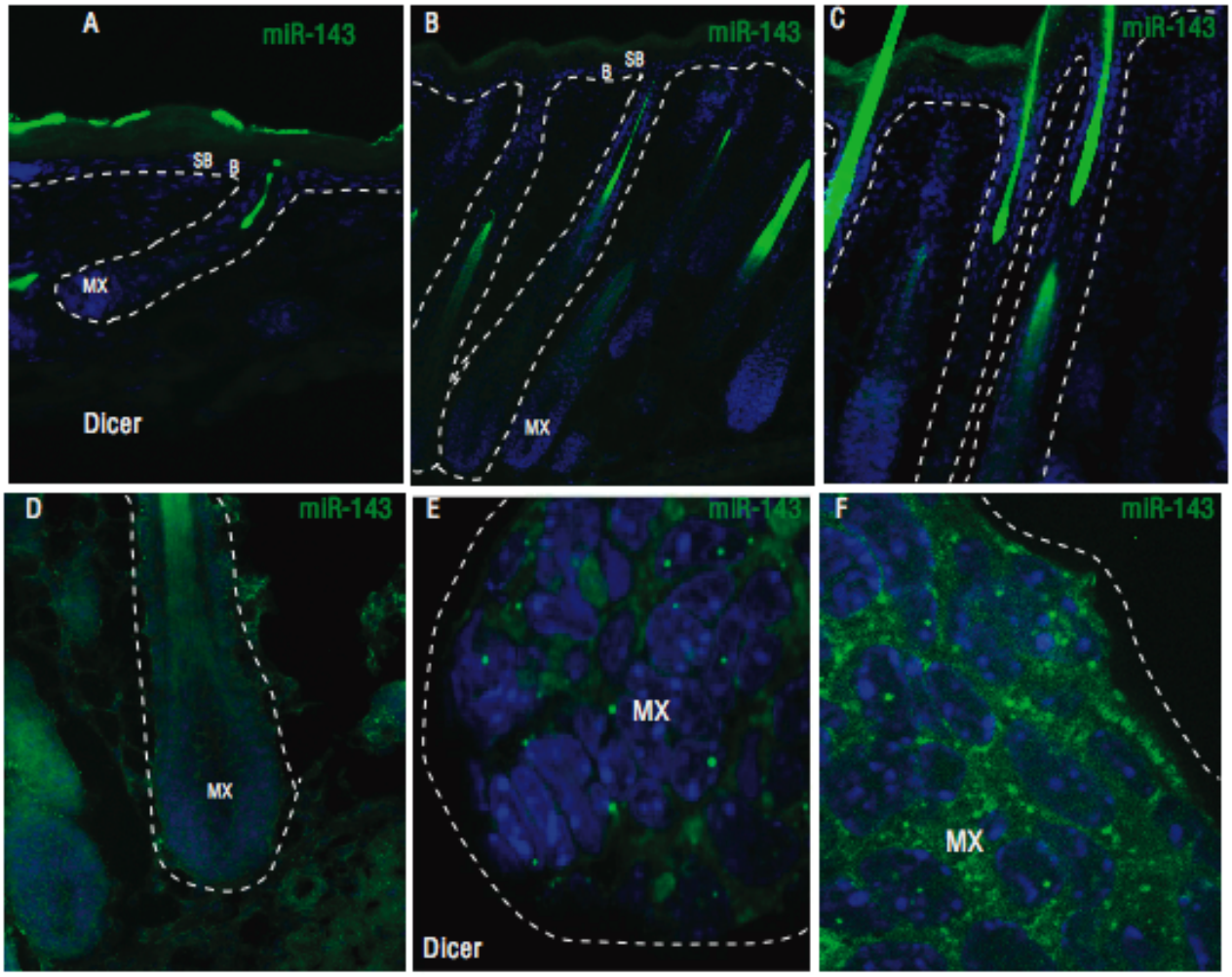

MiR-143 Expression in Postnatal day 4 (P4) mice: A) Negative control Dicer: No expression as expected. B) Epidermis and hair follicle at 10x magnification which shows minimal expression of miR-143 localized to the suprabasal level. The matrix cells are dense and in this image, the signal appears to be masked. C) Epidermis at 20x magnification showing minimal expression of miR-143 localized to the suprabasal cells. D) Matrix at 20x magnification indicates possible expression of miR-143 in the matrix. The background noise is high in this image. E) Confocal image of Dicer control at 100x magnification: This image is used to determine the background fluorescence. The bright green dots are non-specific

signals as they are localized in the nucleus and cytoplasm (mature microRNAs are located in the cytoplasm). F) Confocal image of wild type back skin at 100x magnification confirming uniform expression of miR-143 in the matrix

C. Embryonic Expression

MiR-143 is not only expressed in skin tissue but in embryonic tissues as well. Embryonic tissue was isolated from mice at embryonic day 17.5 (E17.5). Both NBT/BCIP and FISH indicated that there is expression of miR-143 in the heart and possibly the stomach. Further validation of expression in the stomach is needed because there could be endogenous expression of alkaline phosphatase and peroxidase in this tissue. Alkaline phosphatase and peroxidase are the enzymes that are attached to the anti-DIG probes that catalyze the reaction signals during the NBT/BCIP *in situ* hybridization. NBT/BCIP and FISH indicate that miR-143 is expressed in the suprabasal layer of the epidermis and in the developing hair follicles of embryonic tissue (Figure 3.7 Panels A, B, C, D, G, and H). Expression is also seen in the epithelium of the stomach lining (Figure 3.7 Panels E and F) and smooth muscle (Figure 3.7 Panel I and J) in the heart.

Figure 3.7

MiR-143 Embryonic Expression

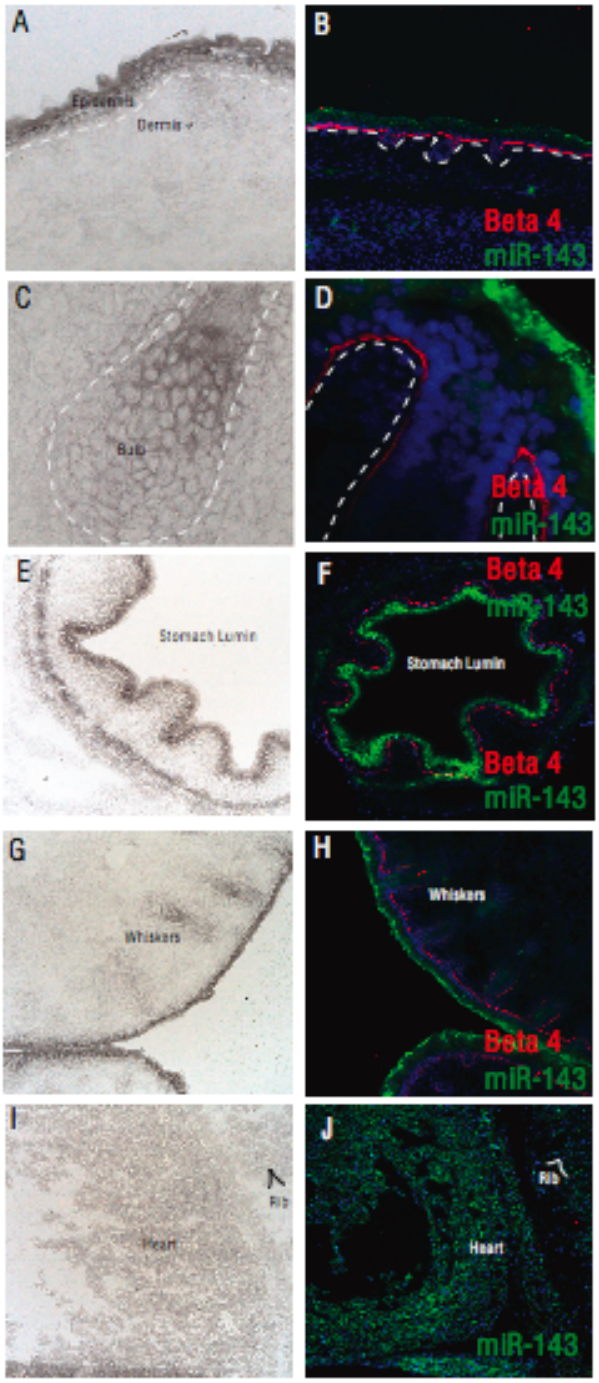

Figure 3.7:
Embryonic tissue was isolated from E17.5 mice. Panels A, C, E, G, I: NBT/BCIP, Panels B, D, F, H, J: FISH.

A, B: MiR-143 expression is seen in the epidermis, specifically in the suprabasal layer.

C, D: MiR-143 is expressed in the bulb region in conjunction with minimal expression in the suprabasal layer.
E, F: This is a cross-sectional view of the embryonic tissue in the stomach. MiR-143 expression is localized to the outer most epithelial layer.
G, H: Whisker development shows expression of miR-143 in the hair follicles and minimally in the epidermis.
I, J: The tissue to the left side is the heart/smooth muscle of the heart. To the right is a rib. MiR-143 expression is localized throughout the tissue presumably in the smooth muscle.

Section 3: MiR-125b Expression Pattern

Figure 3.8

Illustration of Observed Expression

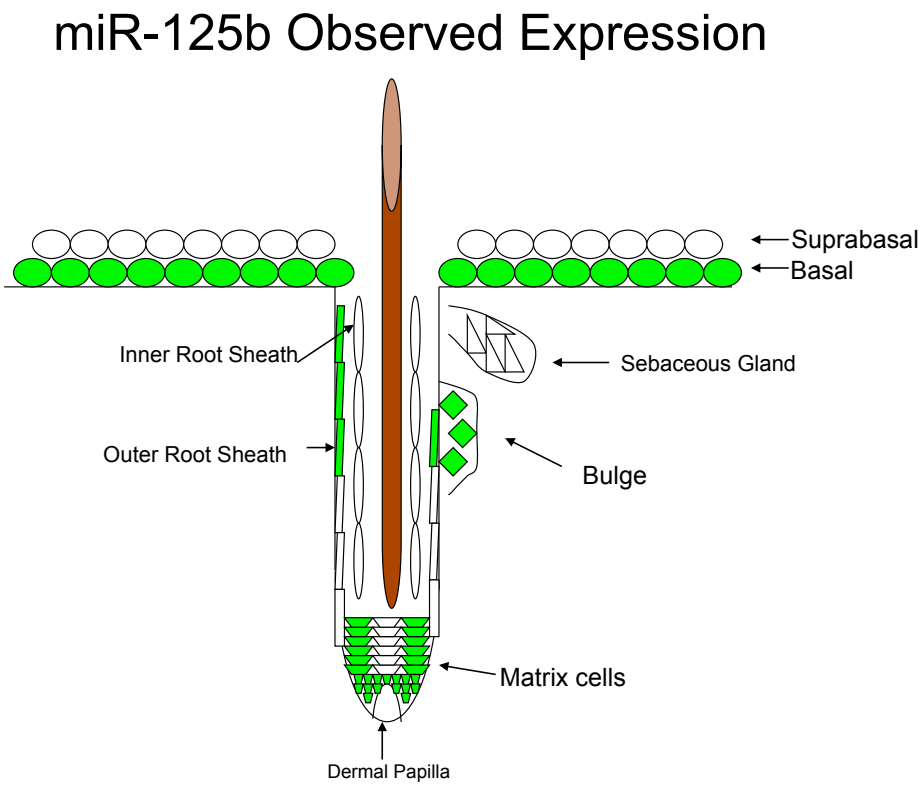

A. NBT/BCIP in situ hybridization

MiR-125b is less abundantly expressed in the skin compared to miR-203. Published data indicates that miR-125b is expressed in the upper outer root sheath, bulge region, and in the basal layer of the skin (Zhang et al., 2011). My data supports these findings and also indicates that miR-125b is also expressed in the tip of the matrix. When images of *in situ* hybridizations for miR-125b using NBT/BCIP are overexposed the miR-125b signal in the matrix is above the background of the negative control (Figure 3.9)

Figure 3.9

MiR-125b NBT/BCIP

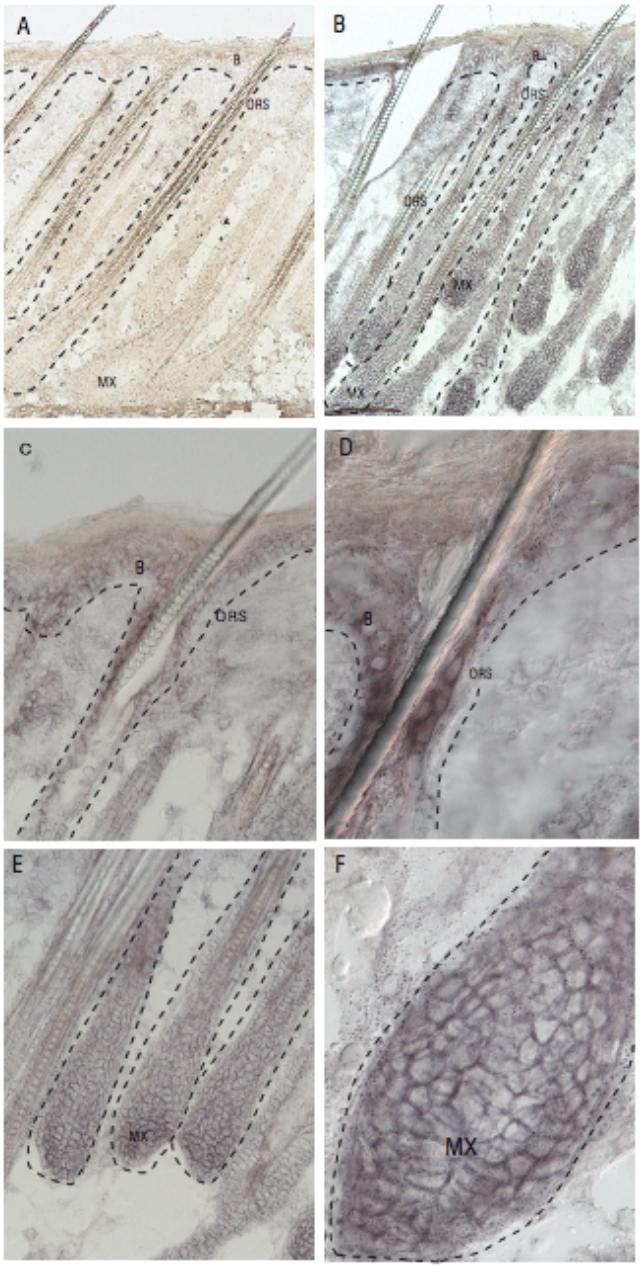

Figure 3.9
The tissue in this figure was isolated from the back skin of P6 mice.
A) Negative control at 10x magnification to detect background noise in these images. The background noise is high indicating overdevelopment.
B) Epidermis and hair follicle at 10x magnification: indicating miR-125b expression in the epidermis, the outer root sheath, and the tip of the matrix.
C) Epidermis at 20x magnification: miR-125b expression is seen in the outer root sheath close to the epidermis with the signal being stronger in the basal cells of the epidermis.
D) Epidermis at 63x magnification: indicating miR-125b minimal (possible non-specific) expression in the suprabasal layer and strong expression in the basal layer.
E) Matrix at 20x magnification: indicating some miR-125b expression in the tip of the matrix.
F) Matrix at 63x magnification indicating: miR-125b expression at the tip of the matrix. The signal decreases in intensity at the center of the matrix.

Section 4: MiR-205 Expression Pattern

Figure 3.10

Illustration of Observed Expression

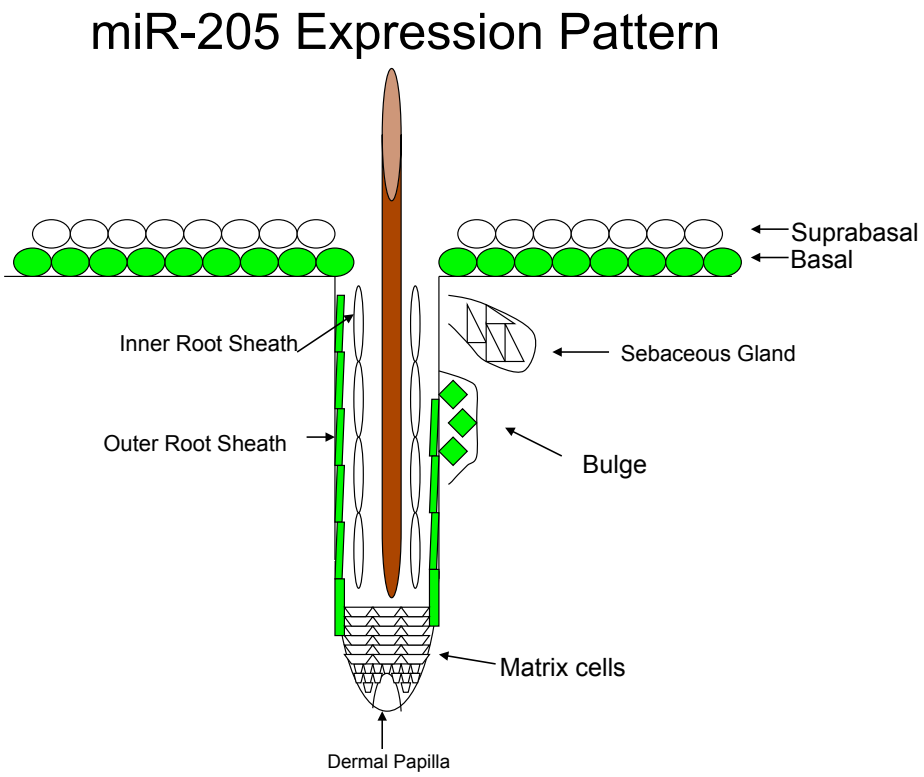

A. NBT/BCIP in situ hybridization

MiR-205 is expressed in undifferentiated skin cell lineages including the basal layer and outer root sheath. The images below show the expression patterns of miR-205 using NBT/BCIP *in situ* hybridization and FISH.

Figure 3.11

MiR-205 NBT/BCIP

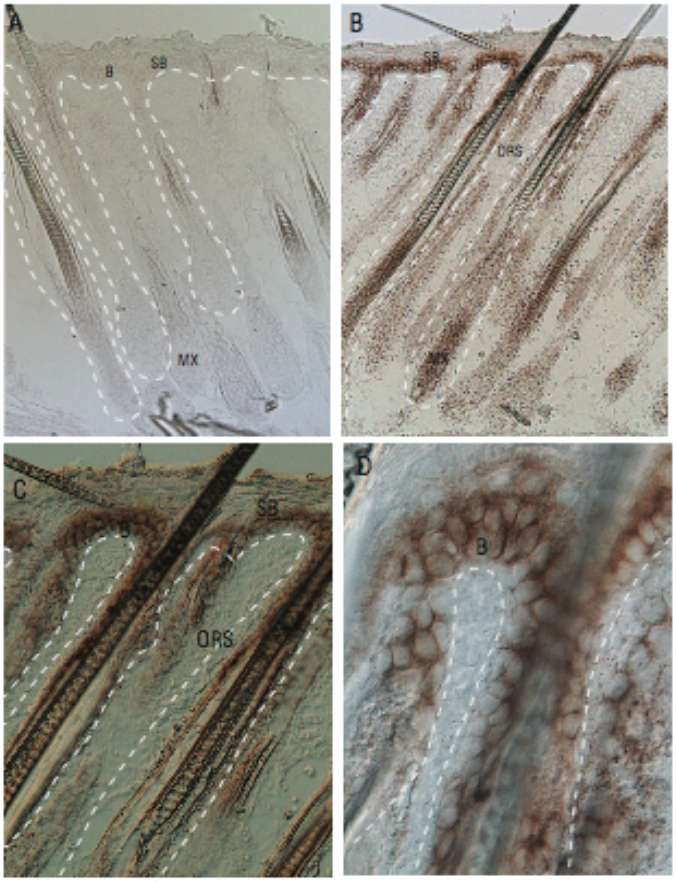

Figure 3.11
Tissue was isolate from the back skin of P6 mice.
A) Negative control at 10x magnification to detect background noise in these images
B) Epidermis and hair follicles at 10x magnification: indicating miR-205 expression in the epidermis, and hair follicle.
C) Epidermis at 20x magnification: miR-205 expression is seen in both layers of the epidermis and the outer root sheath.
D) Epidermis at 63x magnification: indicating miR-205 expression in the basal layer with possible non-specific expression in the suprabasal layer.

B. Fluorescent in situ hybridization/ Confocal Images

Postnatal expression of miR-205 has been characterized in epidermal mouse tissue; however no expression pattern has been determined for embryonic hair follicle morphogenesis. MiR-205 is actively expressed in all stages of hair follicle morphogenesis: two layer epidermis, hair peg, hair germ, and hair follicle. FISH images were generated using confocal microscopy to enhance localization detail of the miR-205 signal. Samples were co-stained with beta-4 integrin (red) to show the separation between the epidermis and dermis. The nucleus is stained (blue) with Hoechst dye and miR-143 is seen in green.

Figure 3.12

MiR-205 Fluorescent *in situ* hybridization

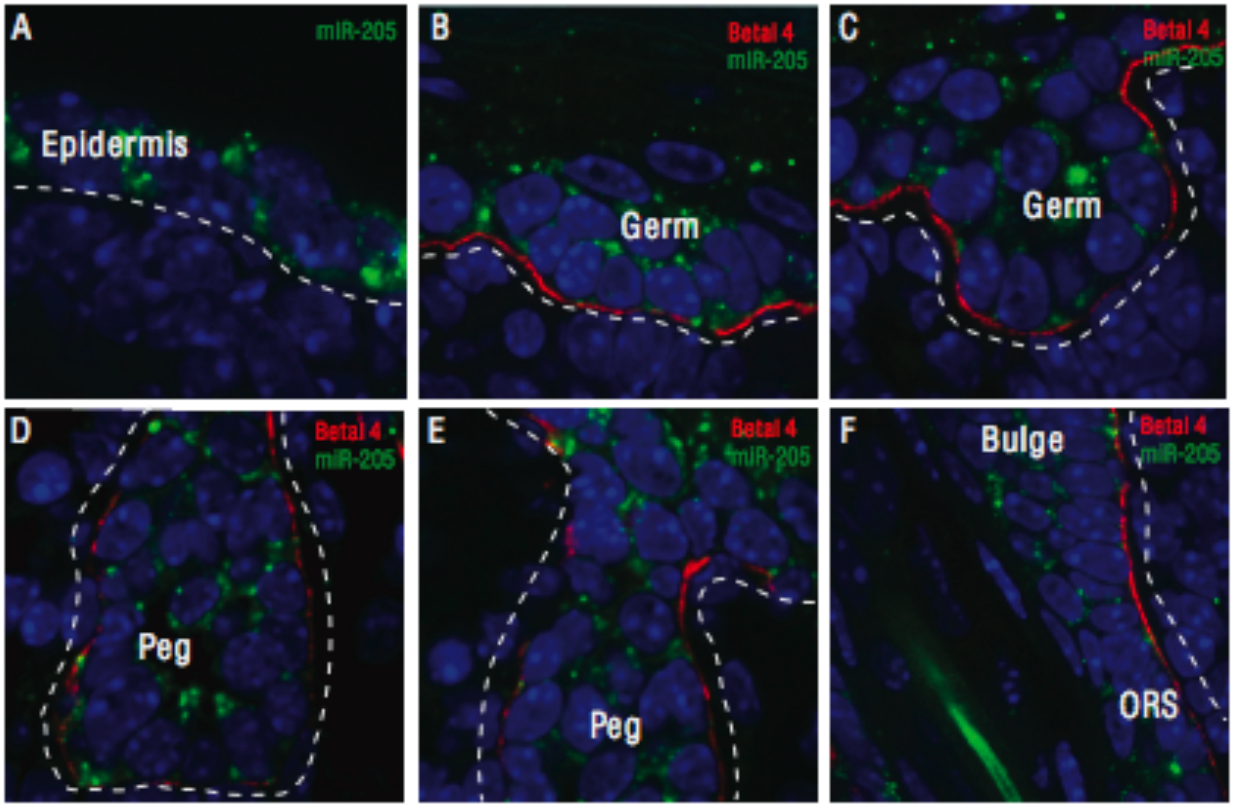

Tissue was isolated from mice at embryonic day 14.5 (14.5): A) Epidermis 100x magnification: shows expression of miR-205 in early epidermal development. B) Invaginating hair germ at 100x magnification: shows miR-205 expression as hair follicles begin to form. MiR-205 expression is seen in the basal layer as the epidermis invaginates into dermis. C) Invaginating hair germ at 100x magnification: miR-205 expression is seen as the hair germ matures. D) Developing hair peg at 100x magnification: indicates miR-205 expression in the hair peg extending down into the dermis E) Developing hair peg including epidermis at 100x magnification: demonstrating miR-205 expression in the epidermis residing in the basal layer. F) Upper hair follicle at 100x magnification: the bulge region is located in the outlined follicle toward the top of the image and miR-205 expression is clearly seen here as well as in the outer root sheath.

C. Embryonic Expression

MiR-205 is expressed in other embryonic tissues in addition to the skin including the liver, forebrain, sinuous, and eye region.

Figure 3.13

MiR-205 Embryonic NBT/BCIP

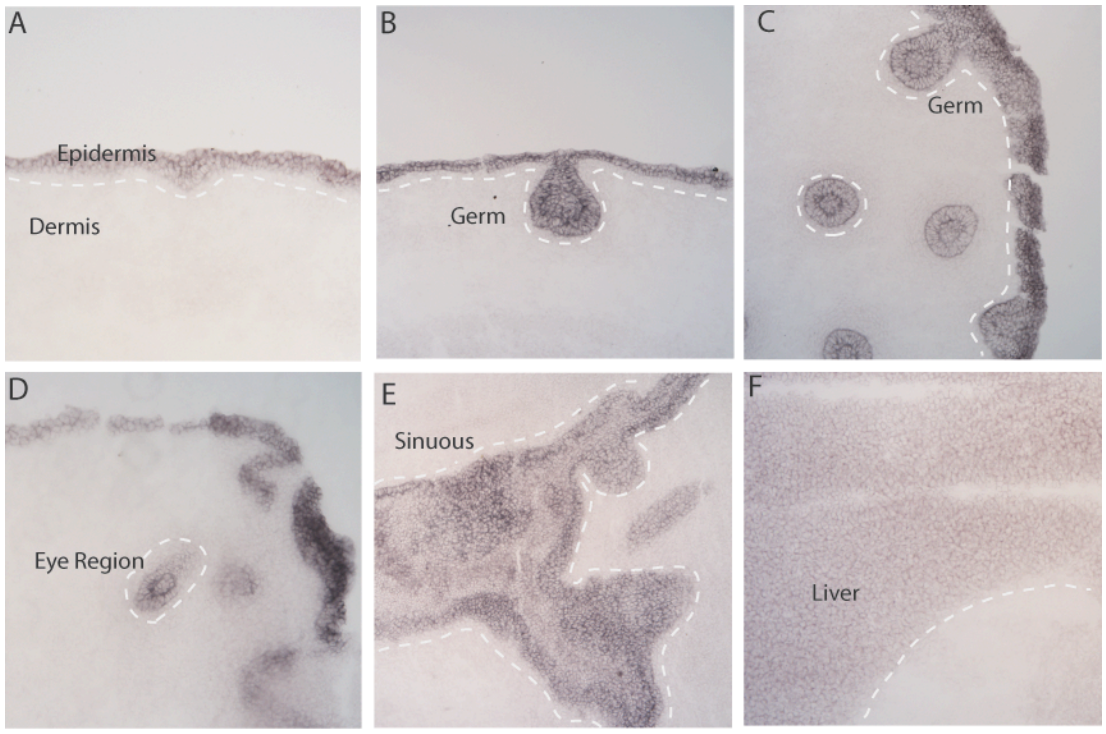

These samples were isolated from embryonic day 14.5 mice. A) Epidermis at 10x magnification: shows that miR-205 expression is localized to the epidermis. B and C) Developing hair follicles at 10x magnification: shows that miR-205 is expressed in epidermal back skin (B) and facial epidermis forming whiskers (C). D) Eye region at 10x magnification: shows that miR-205 is highly expressed here. E) Sinuous at 10x magnification: shows that miR-205 is highly expressed in the sinuous and is localized to the outer lining with decreasing signal toward the center. F) Liver at 10x magnification: shows miR-205 is uniformly and minimally expressed in the liver.

D. Quantification of miR-205 tissue exploration

Using NBT/BCIP in situ hybridization, miR-205 is expressed in other embryonic and postnatal tissues in addition to the skin. To verify the observed expression by NBT/BCIP, rt-qPCR was used to quantify relative microRNA abundance. Figure 3.14 and 3.15 show the relative fold expression of miR-205 expression in various tissues. The internal controls for this experiment were the endogenous microRNAs expressed in all cells, sno25 and let7.

Figure 3.14

Relative Expression of miR-205 in Different Tissue Types in Postnatal Day 10 Mice

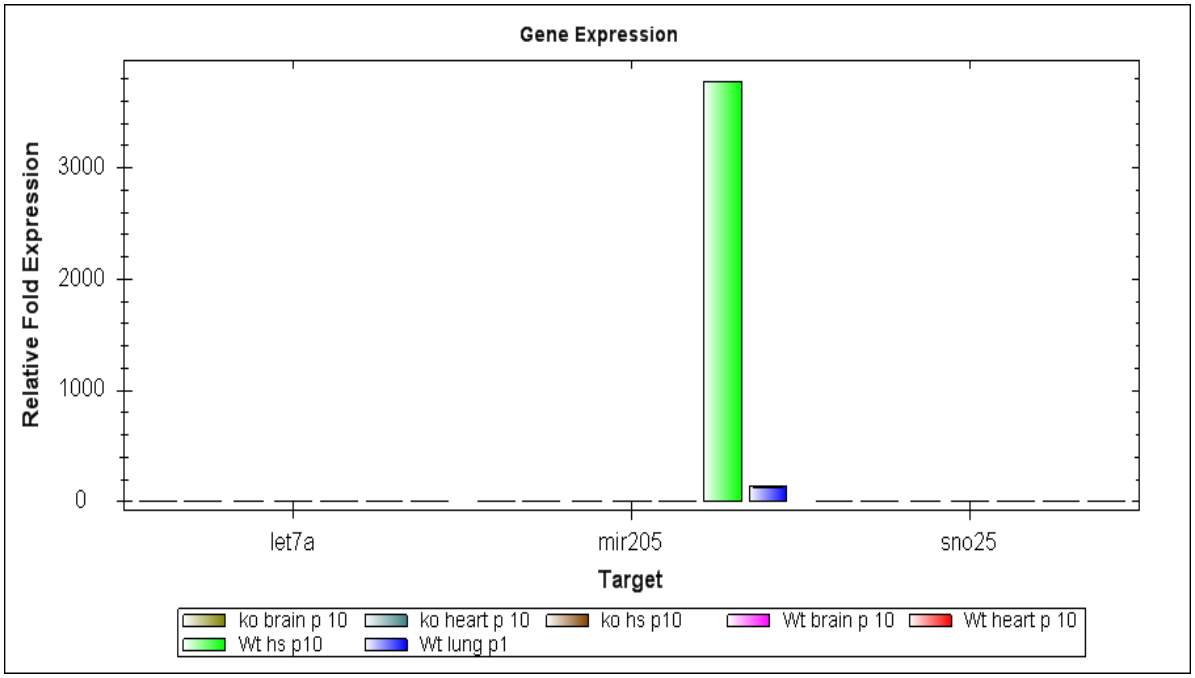

MiR-205 is abundantly expressed in the skin and minimally expressed in the lungs. The linear Y-axis shows the abundance and relative expression of miR-205

Figure 3.15

Relative Expression of miR-205 in Different Tissue Types in Postnatal Day 10 Mice

(Log Base 2)

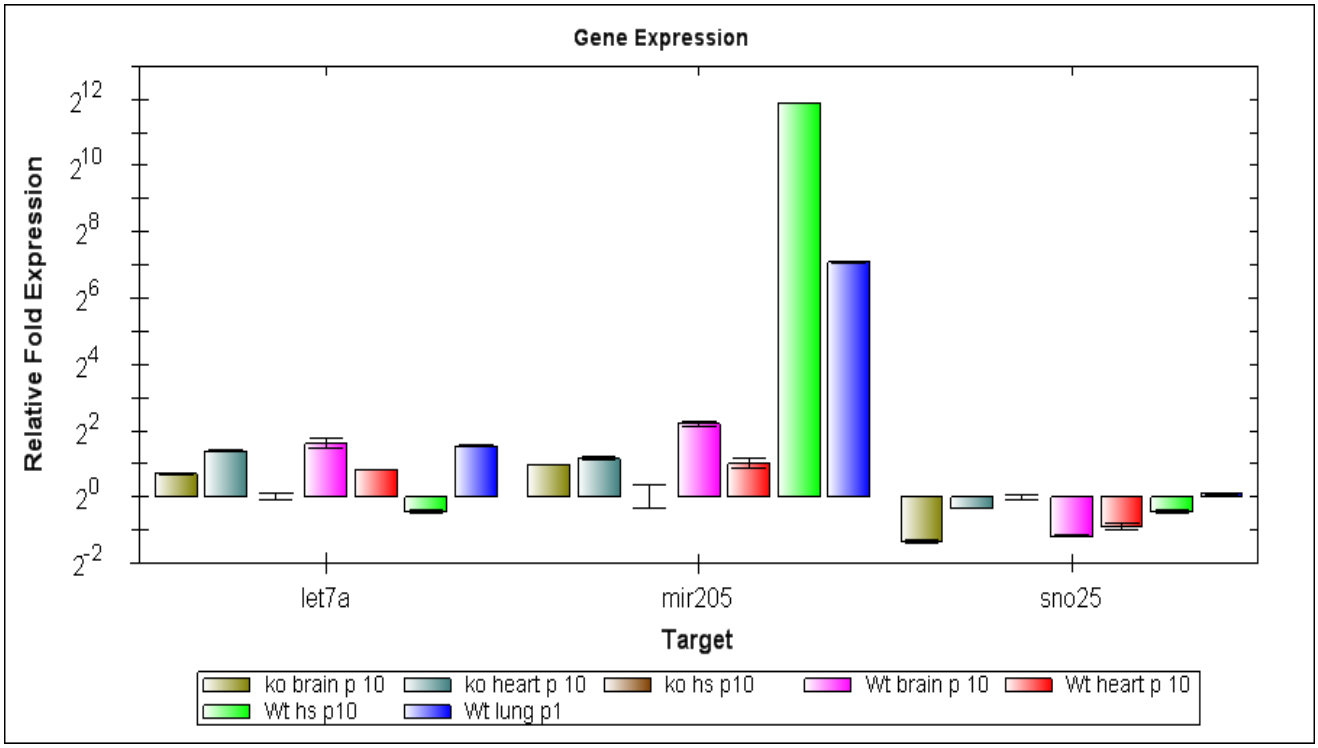

Using a log scale to diagram the expression of miR-205, additional expression in the brain and heart are observed. When the expression of miR-205 in wild type tissues is compared to the same tissue in the knock out mice, the only observable difference in miR-205 expression is seen in the skin and lung tissue.

Section 5: Luciferase Assay

Luciferase assays were used to test predicted DNA sequences thought to contain promoter activity. DNA was selected based on ChIp-Seq data and Evolutionary conservation. Three DNA sequences were tested (Constructs A, B, and C).

ChIP-Seq is a method that is able to sequence DNA bound to different proteins. In this case, the interaction between histones and DNA is targeted. Histones are proteins that bind to

DNA and wind it up in a spool to condense it. There are various chemical marks on the histones that can identify different biological functions. For example on histone 3 lysine residue 4, trimethylation marks DNA regions that are used for promoters. Elongation can be identified by methylation on histone 3 lysine reside 36. ChIP-Seq is therefore able to correlate the DNA sequence with the modifications of the histones. This makes it accessible to compare the histone modifications to annotated genes.

Figure 3.16 (Li Wang, Yi Lab)

ChIP-Seq for miR-205

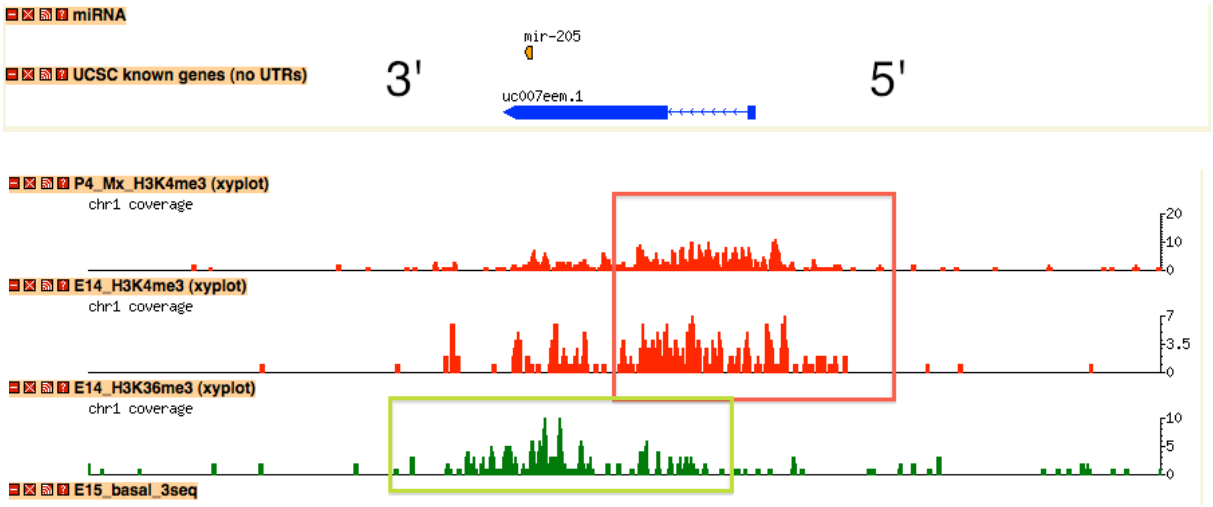

ChIp-Seg for Histone 3 Lysine 4 trimethylation (H3K4me3) is in red. H3K4me3 peaks can predict promoter regions. The first H3K4me3 bar is ChIP-Seg from P4 mice and the second bar is from E14 mice. This data predicts that there is not one distinct promoter region as shown by the multiple peaks at the 5' end of the EST (blue). The green peaks are Histone 3 Lysine 36 trimethylation marks (HeK36me3), this identifies active elongation of transcription. The H3K36me3 are normal because peaks are seen after transcription stars and close to miR-205. The EST is shown in blue (5' is to the right, 3' to the left). MiR-205 is transcribed from right to left and shown in yellow above the blue EST.

A. Construct A

Figure 3.17

Luciferase Expression driven by Construct A (8.3 kb region)

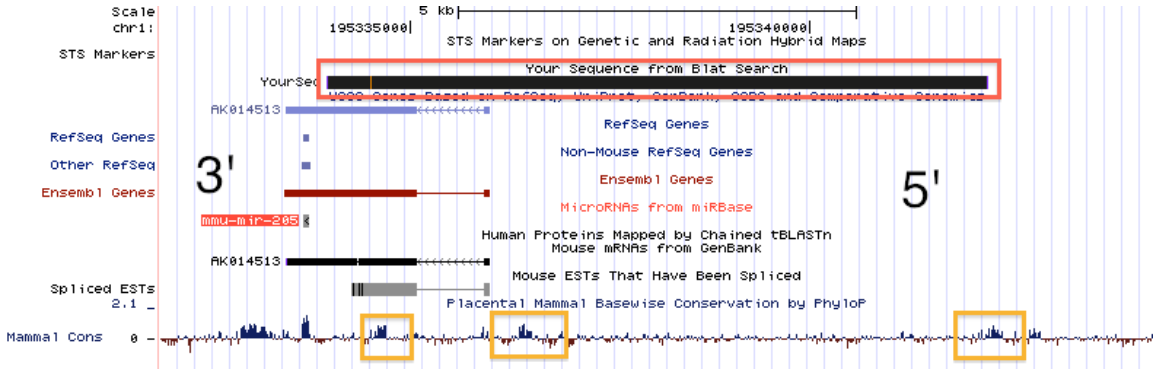

This figure shows the conservation of important DNA sequences surrounding miR-205 gene. ChIP-Seq shows data suggests some promoter activity in this region. The black striped bar boxed in red, shows the region of DNA used to create Construct A. There are peaks of conservation at the transcriptional start site, slightly upstream of the transcription start site, and in the second exon all highlighted in yellow. These conservation peaks suggest that these DNA sequences are conserved through out mammals.

When this DNA sequence was used in a luciferase assay, there was slight activity when normalized to pGL3 Basic. PGL3 Control (SV40 promoter) and pGL3 203 (miR-203 active promoter) were used as positive controls to compare luciferase activity.

Figure 3.18

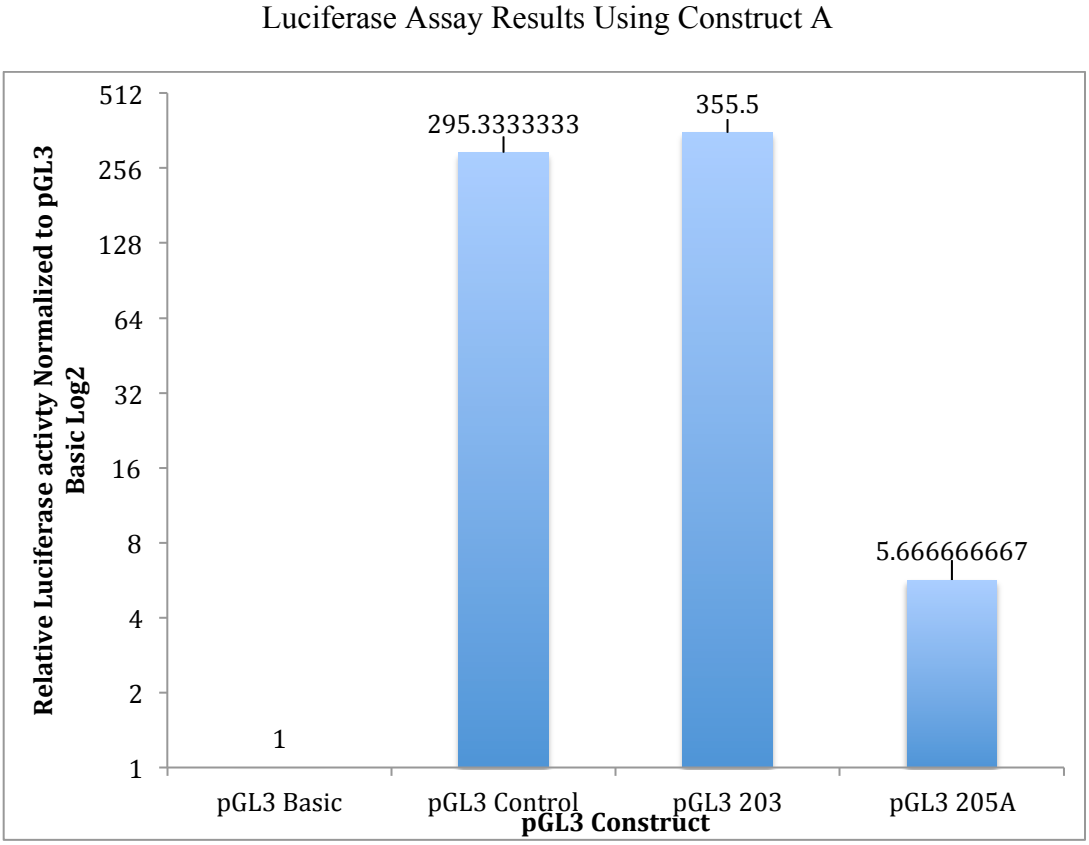

The graph in Figure 3.18 shows the relative expression of the promoter construct A when normalized to the pGL3 Basic construct, which lacks a promoter insert. PGL3 205A shows minimal luciferase activity suggesting construct A does not contain an active promoter region. PGL3 Control and pGL3 203 show high luciferase activity.

Figure 3.19. Relative Florescence Unit (RFU) Values for Controls and Construct A

Construct	Luciferase RFU	Renilla RFU	Ratio L:R
pgl3 basic well1	3825	20142260	0.0002
pgl3 basic well2	5944	26310040	0.0002
pgl3 basic well3	5596	29653018	0.0002
pgl3 control well1	1510067	30505442	0.0495

pgl3 control well2	2990536	50307760	0.0594
pgl3 control well3	2168345	31742078	0.0683
pgl3 203 promo10 well1	1855597	25564540	0.0726
pgl3 203 promo10 well2	2007495	25167350	0.0798
pgl3 203 promo10 well3	1496436	24556158	0.0609
pgl3 205 well1	13639	9840051	0.0014
pgl3 205 well2	18559	19276952	0.001
pgl3 205 well3	15542	15332891	0.001

The actual luciferase RFUs from the dual luciferase assay in each of the constructs is shown in Figure 3.19. The RFU from the renilla luciferase should be relatively constant for each sample and between each of the constructs.

B. Construct B

Construct B contain some of the same DNA as construct A, however this DNA sequence is further 5' and small than construct A. Construct B is located in the middle of the first intron (figure 3.20).

Figure 3.20

Luciferase expression driven by Construct B (4.5 kb region)

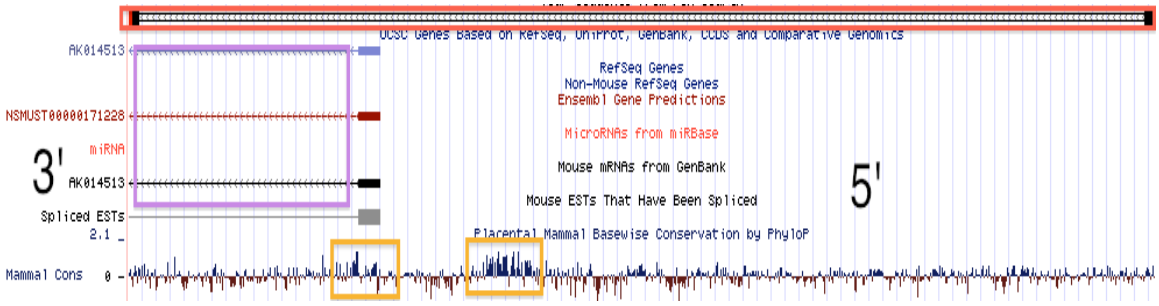

This figure shows the conservation of important DNA sequences surrounding miR-205 gene. ChIP-Seq shows data suggests some promoter activity in this region. The black striped bar boxed in red, shows the region of DNA used to create construct B. There are peaks of conservation at the transcriptional start site and slightly upstream of the transcription start site highlighted in yellow. These conservation peaks suggest that these DNA sequences are conserved through out mammals. Notice construct B is located 5' of Construct A (Figure 3.17) and includes DNA in the intron showed in purple.

This DNA region was used in a luciferase assay to determine its promoter activity. As shown in Figure 3.21, construct B negatively affects luciferase activity and suggests that this DNA fragment does not drive the expression on miR-205.

Figure 3.21

Luciferase Assay Results Using Construct B

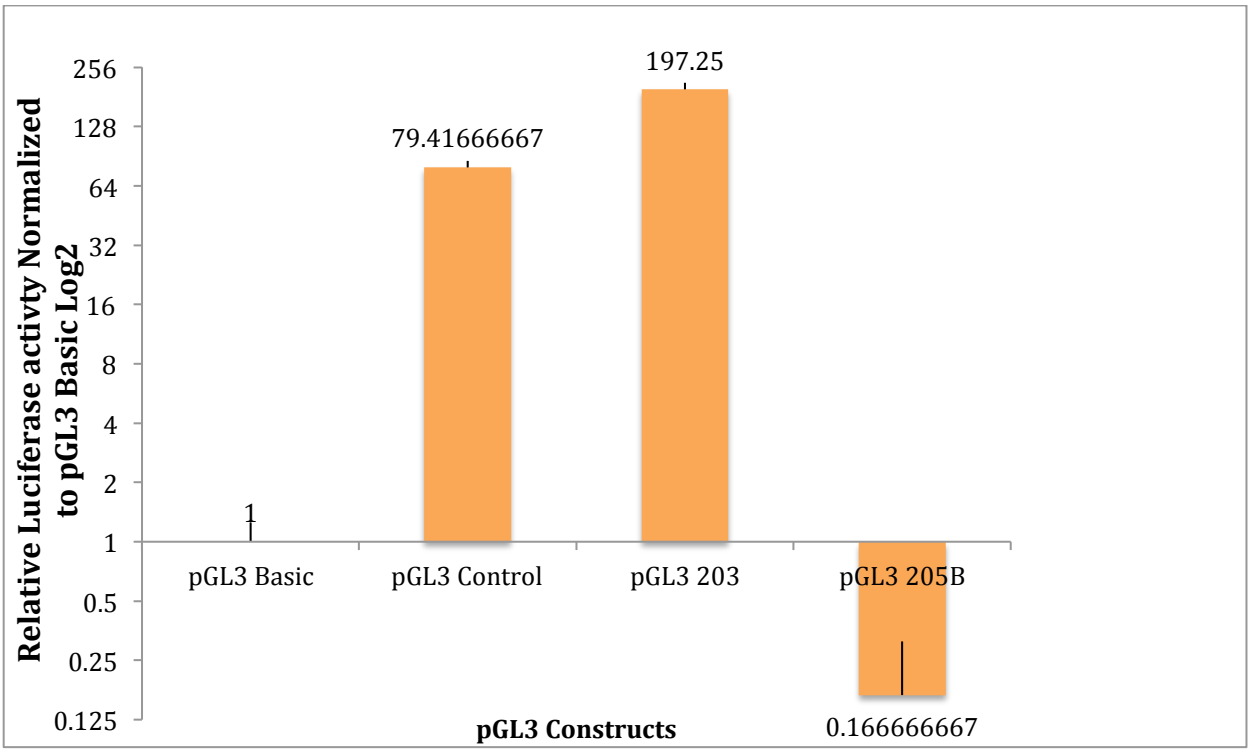

The graph in Figure 3.21 shows the relative expression of the promoter construct B when normalized to the pGL3 Basic construct, which lacks a promoter insert. PGL3 205B has less luciferase activity thank pGL3 Basic (negative control). This suggests that the intron could negatively affect the

translation of luciferase gene if it is not spliced (normally introns are cut out before translation). PGL3 Control and pGL3 203 show high luciferase activity.

Figure 3.22

RFU Values for Controls and Construct B

Construct	Luciferase RFU	Renilla RFU	Ratio L:R
pgl3 basic	12372	39099516	0.0003
pgl3 basic	9410	19983272	0.0005
pgl3 basic	14030	34674184	0.0004
pgl3 control	1034377	30009482	0.0345
pgl3 control	1126704	36774684	0.0306
pgl3 control	776183	25665536	0.0302
pGL3 203	2488136	28746380	0.0866
pGL3 203	1791440	23917484	0.0749
pGL3 203	1704125	22659524	0.0752
pgl3 205B	771	14302725	0.0001
pgl3 205B	323	9004732	0
pgl3 205B	1062	14369534	0.0001

The actual luciferase RFUs from the dual luciferase assays in each of the B constructs is shown in Figure 22. The Relative Flourescence Unit (RFU) from the renilla luciferase should be relatively constant for each sample and between each of the constructs.

C. Construct C

This DNA sequence is important because it will show if the DNA downstream of construct C were causing the minimal luciferase activity. Construct C included the transcriptional start site and DNA upstream of that. No DNA downstream of the transcription start site is included (Figure 3.23).

Figure 3.23

Luciferase expression driven by Construct C (2.7 Kb region)

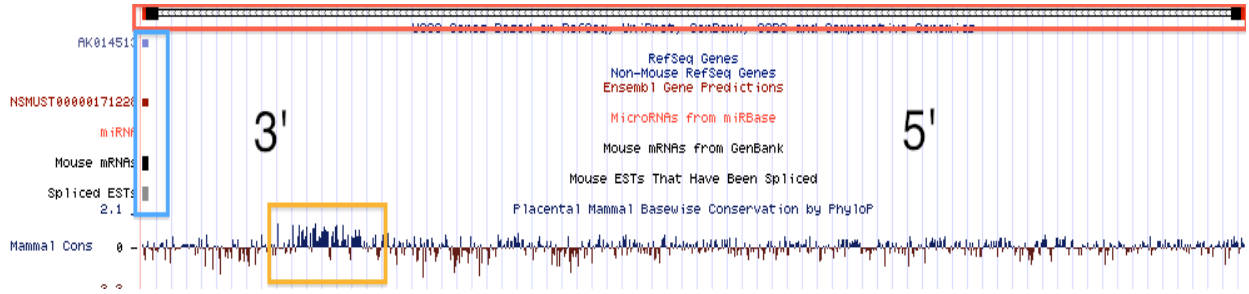

This figure shows the conservation of important DNA sequences upstream of miR-205 gene. ChIP-Seq shows data suggests some promoter activity in this region. The black striped bar boxed in red, shows the region of DNA used to create construct B. There are peaks of conservation slightly upstream of the transcription start site (blue) highlighted in yellow. These conservation peaks suggest that these DNA sequences are conserved through out mammals. Construct C starts at the transcriptional start site boxed in blue. This is the beginning of the first exon.

This DNA region was used in a luciferase assay to determine its promoter activity. As shown in Figure 3.24, construct C has minimal luciferase activity. Both construct A and C were used to compare general luciferase activity in the same experimental settings. Figure 3.24 shows that there is not a large different between the two constructs and that they have minimal luciferase activity compared to pGL3 Basic.

Figure 3.24

Luciferase Assay Results Using Construct C

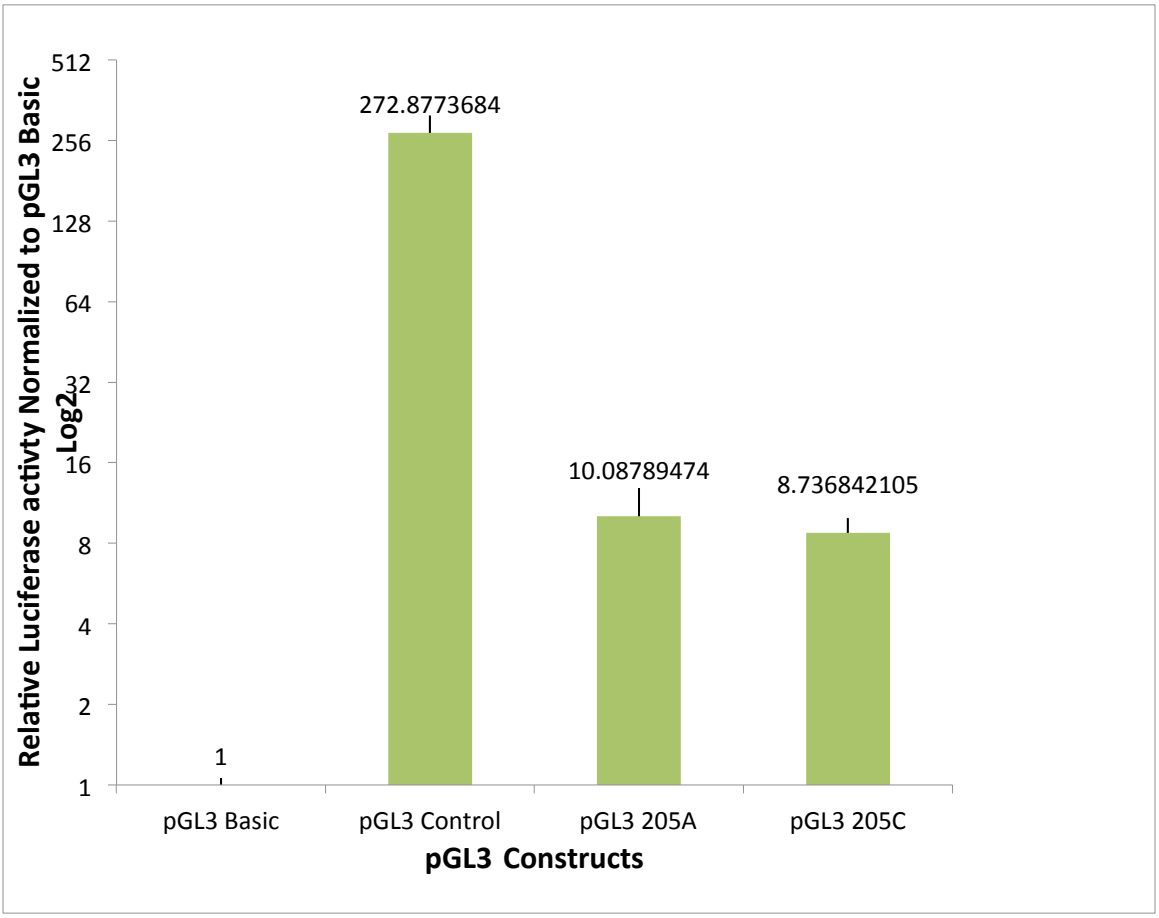

The graph in Figure 3.24 shows the relative expression of the promoter C constructs when normalized to the pGL3 Basic construct, which lacks a promoter insert. The luciferase activity of construct A compared to construct C shows that pGL3 205A has1.4 fold higher activity than pGL3 205C. The pGL3 control vector (SV40 promoter) is much higher than pGL3 205A and C promoter regions. This data suggests that the A and C constructs have similar activty levels, which are low compared to the pGL3 Control.

Figure 3.25

RFU Values Comparing Controls, Construct A, and C

Construct	Luciferase	Renilla	Ratio L:R
pGL3 Basic	58561	34906128	0.0017
pGL3 Basic	53682	28542632	0.0019
pGL3 Basic	38285	19927378	0.0019
pGL3 Control	14214210	26453000	0.5373
pGL3 Control	15047384	25522226	0.5896
pGL3 Control	17376206	40552072	0.4285
pGL3 205A	270221	14268403	0.0189
pGL3 205A	166481	6831116	0.0244
pGL3 205A	356806	25131206	0.0142
pGL3 205C	133942	9216099	0.0145
pGL3 205C	141647	7508077	0.0189
pGL3 205C	277038	16905292	0.0164

The actual luciferase RFUs from the dual luciferase assays in A and C constructs is shown in Figure 25. The Relative Flourescence Unit (RFU) from the renilla luciferase should be relatively constant for each sample and between each of the constructs.

D. 293T Luciferase Assay

Construct C was also transfected into human embryonic kidney cells (293T cells, also referred to as BOC cells). Using Northern Blot assays, the Yi lab has determined that miR-205 is not expressed in these cells, but miR-203 is expressed. Since miR-205 is not expressed in this cell line, any luciferase activity will from pGL3 205C will demonstrate baseline detection of this DNA, suggesting it is not an active promoter region.

Figure 3.26

Luciferase Assay Results of Construct C in BOC Cells

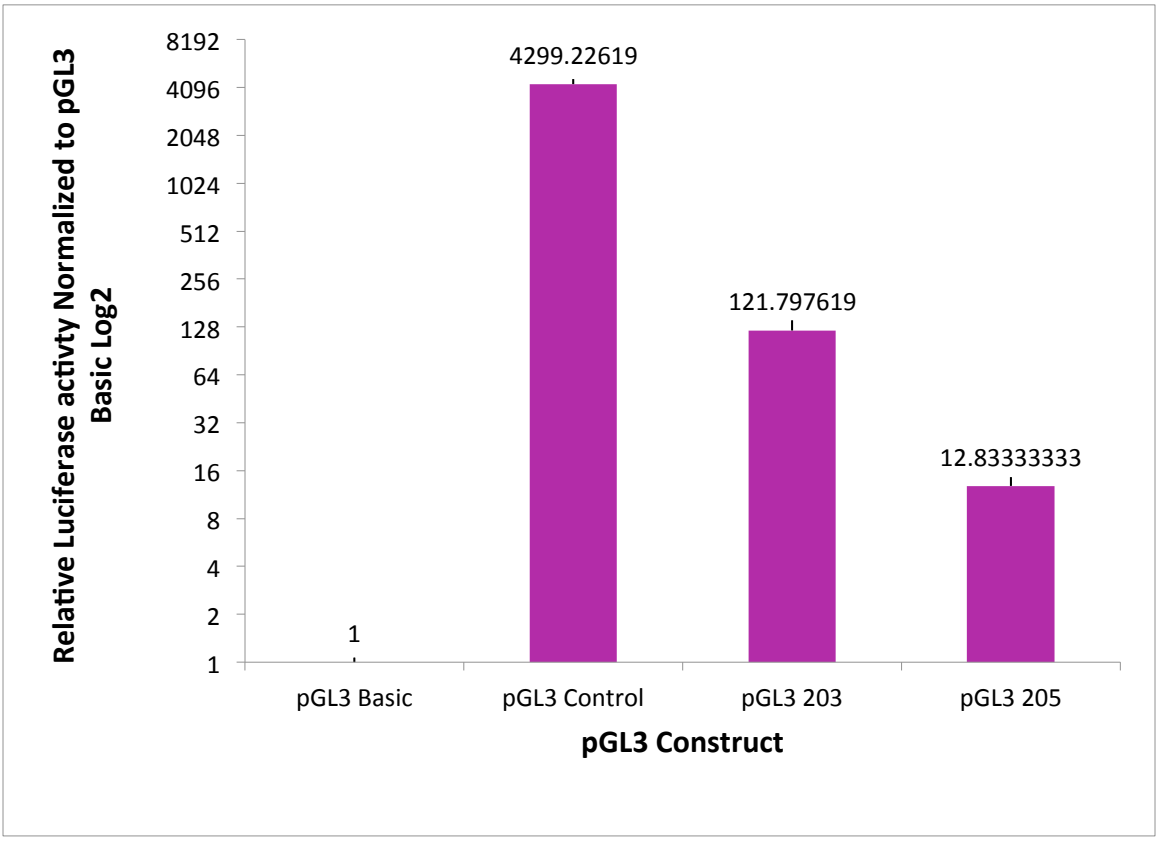

The graph in Figure 3.26 shows the relative expression of the pGL3 203 and 205C when normalized to the pGL3 Basic construct, which lacks a promoter insert. The luciferase activity of. the pGL3 control is much more active in BOC cells than in keratinocytes. Different promoter activity levels for the same construct have been observed in different cell lines. The pGL3 control is 4,177 fold more active than pGL3 203 construct,. This suggests only that SV40 promoters are more avtive in BOC cells compared to keritinocytes. PGL3 203 has higher luciferase activty compared to pGL3 205C. This not only confirms that miR-203 is activte and present in BOC cells, but also shows that pGL3 205C still has about a 13 fold increase in activity when normalized to pGL3 Basic. If pGL3 205C still has minimal activity in BOC cells (where miR-205 is not present) then it can be assumed that this "minimal" luciferase activty does not equate to any promoter activity.

Figure 3.27

RFU Values of Construct C in BOC cells

Construct	Luciferase RFU	Renilla RFU	Ratio L:R
pGL3 Basic	20679	7299181	0.0028
pGL3 Basic	22652	7445225	0.003
pGL3 Basic	19218	7494504	0.0026
pGL3 Control	58142424	5085558	11.4328
pGL3 Control	62676600	4816253	13.0136
pGL3 Control	51325588	4399167	11.6671
pGL3 203	1539185	5139493	0.2995
pGL3 203	2056767	5132919	0.4007
pGL3 203	1030674	3191977	0.3229
pGL3 205	215023	6903867	0.0311
pGL3 205	269783	6573759	0.041
pGL3 205	251319	7046033	0.0357

The actual luciferase RFUs from the dual luciferase assays in pGL3 203 and 205 constructs is shown in Figure 3.27. The RFU from the renilla luciferase should be relatively constant for each sample and between each of the constructs.

Chapter 4: Discussion

To shed light on the role microRNA has in differentiation of stem cells in the skin, the localization and expression patterns for those micro RNAs must be determined. It is known that microRNAs are differentially expressed in the skin. Localization of particular microRNAs in the

skin will suggest a role for their function. *In situ* hybridization studies were used to determine the expression patterns of miR-143, miR-125b, and miR-205 in skin tissue. MiR-203 was used as a positive control in these hybridizations.

Section 1: In Situ Hybridization

Both NBT/BCIP and FISH methods were used to detect microRNA in various epithelial tissues. The hybridization patterns with NBT/BCIP can be utilized to understand the general expression pattern of microRNAs, but overdeveloped samples can show potential non-specific expression. The FISH technique is useful in that it can validate the preferential expression of microRNA seen in NBT/BCIP and can also detect the sub-cellular localization of microRNAs in the samples being tested.

A. MiR-203's Expression Pattern:

MiR-203 has a distinct expression pattern localized to the suprabasal cells in the epidermis as well as to the inner root sheath, sebaceous gland, and pre-cortex fork of the matrix. It is interesting how distinct the expression pattern of miR-203 is in the two adjacent cell types: basal and suprabasal cells indicating that this microRNA might play an important role in the process of differentiation, or be a marker for differentiated cells.

MiR-203 is mainly expressed in differentiated cell types (Yi et al., 2008). To determine the expression pattern of miR-203 in hair follicles, Postnatal day 6 mice (P6) were used. At this age the hair follicles are established but have not started cycling through the hair stages. The bulge region in the skin of mice at this age is difficult to visualize without co-staining because the bulge region is still developing and is small in size. The bulge region typically becomes apparent before the first telogen. MiR-203 served as a positive control in many of these experiments because it is abundant in the hair follicle and epidermis.

B. MiR-143 Expression Pattern:

MiR-143 expression is less abundant than miR-203 as analyzed by small RNA cloning frequency (Yi et al., 2006). MiR-143 is expressed in matrix cells and possibly suprabasal cells. Cells in the matrix are considered to be transit-amplifying (TA) cells, which means they are in the transition between undifferentiated and differentiated cells. These cells are highly proliferative and actively differentiating. Studying expression patterns of microRNAs in skin tissue can provide insights into the molecular steps leading to differentiation.

Using the results from NBT/BCIP, it is apparent that miR-143 expression is much less abundant than miR-203 and miR-205. Analysis of NBT/BCIP patterns reveals miR -143 expression in the matrix and possibly the suprabasal layer, but this needs to be confirmed FISH.

This expression of miR-143 in the matrix is prevalent in P4-P6 mice confirmed by FISH and analyzed with confocal microscopy. The FISH method indicates that there is some signal for miR-143 in the suprabasal cells, which could be due to non-specific expression. The negative control for these FISH experiments was a Dicer knock-out, which would not produce any signal for microRNA since Dicer is required for microRNA biogenesis. FISH images with tissue from the Dicer knock-out shows non-specific expression in the stratus corneum. This layer often imitates high expression even though it is actually composed of dead cells. An examination of the area below the stratus corneum indicates that the suprabasal layer contains minimal expression of miR-143. The difference in the intensity of the miR-143 signal compared to the Dicer knock-out is significant when looking at matrix cells. MiR-143 has a much higher signal in the wild type tissue. Therefore, confocal images confirm that miR-143 is expressed in the matrix,

Ideally, the expression any microRNA in the dicer knock-out should be non-existent. However, there were minimal non-specific signals indicated by the presence of bright green dots scattered in the nucleus and cytoplasm. MicroRNAs are localized in the cytoplasm, which suggests that these dots are non-specific signals in the Dicer knock-outs. The remaining background noise can be a result of experimental procedures including hybridization temperatures, stringency of washes, and amplification times.

MiR-143's expression was also explored in embryos that were 17.5 days old (E17.5). At this age, there are several different stages of hair follicles developing in the embryo. MiR-143 was expressed in the suprabasal layer of multi-cellular back skin and belly skin. Hair bulbs were examined at 63X magnification and the expression of miR-143 localized to the suprabasal layer with some expression in the outer root sheath.

MiR-143 expression was seen in other tissues isolated from embryos at day 17.5 including smooth muscle in the heart and epithelial tissue in the gastrointestinal tract (Cordes et al., 2009) (Clape et al., 2009). The digestive and gastrointestinal tract showed miR-143 expression from the mouth though the anus.

The gastrointestinal and digestive tract has endogenous phosphatase and peroxidase activity, which are used by the digestive system to break down food. These enzymes are also used for detection in *in situ* hybridization methods, which could explain the seemingly high miR-143 expression in this tissue. Northern blots and RT-qPCR could be done to verify the intensity of the expression of miR-143 in the gastrointestinal epithelium.

MiR-143 is specifically expressed in matrix cells. This population of cells is distinct from other epithelial cells because they are actively replicating and differentiating. MiR-143 has been shown to play a role in the differentiation of smooth muscle cells and adipose tissue (Elia et

al., 2009) (Takanabe et al., 2008). Perhaps the expression of miR-143 in this cell lineage implies that this microRNA is involved in differentiation of stem cells to terminally differentiated cells in multiple tissues.

C. MiR-125b Expression Pattern:

The results show miR-125b expression in the outer root sheath, basal cells, and tip of the matrix cells supporting the recent literature (Zhang et al. 2011). In skin from P6 mice, miR-125b is mainly expressed in undifferentiated cell lineages. The results show that miR-125b is expressed in the tip of the matrix. However, it is difficult to determine the specific sub-cellular expression of microRNAs in the matrix using only the NBT/BCIP hybridization method. It would be useful to see if the tip alone has isolated miR-125b expression, or if this microRNA resides in the outer most layer of the matrix, where the outer root sheath extends.

Recently, miR-125b has been shown to be expressed in the upper outer root sheath, basal cells, and bulge cells (Zhang et al., 2011). Its localization in undifferentiated cell lineages correlates with its proposed function to regulate early bulge stem cells. MiR-125b is thought to regulate the skin stem cells by inhibiting their differentiation. However, miR-125b does not affect the hair follicle stem cell's ability to maintain a population of stem cells and does not prevent those cells from becoming activated under stimulation (waxing) (Zhang et al., 2011).

These data suggest that some microRNAs can target mRNAs responsible for activation or inhibition of differentiation, thus fine-tuning the gene expression of those cells. This fine-tuning could be modulated with potential drugs and treatments that could target stem cell development.

D. MiR-205 Expression Pattern:

MiR-205 has an abundant and distinct spatial temporal expression pattern, which is seen as early as embryonic day 14 (E14). However, this microRNA may be expressed even earlier between embryonic days 10 and 13 (E10-E13). The epidermis starts to form a single layer of cells between E9.5 and E12.5 (Blanpain et al., 2009). The expression of miR-205's characterized expression is localized to undifferentiated cells in contrast to the expression of miR-203. In *in situ* hybridization experiments, the signal for miR-205 is seen in the basal layer, outer root sheath, and bulge cells. MiR-205 is expressed during the morphogenesis of the hair follicle. Using the confocal microscope to examine tissue from wild type P0, miR-205 was localized at the tip of the invaginating hair germ and bulb. It stays localized to the outer root sheath and resides in the bulge region. Therefore, miR-205 is expressed during the development of hair follicles.

In situ hybridization with NBT/BCIP was done with epithelial tissue isolated from wild postnatal mice age (P6). In these samples, miR-205 is still expressed in undifferentiated cell types including basal cells and less abundantly in the outer root sheath and matrix cells. The expression of miR-205 is likely to be initiated between E10 and E14, as the epidermis develops hair follicles; miR-205 expression is abundant on the leading edge of hair germs as they invaginate into the dermis. Later when hair follicles are still developing, miR-205 is expressed in undifferentiated cell lineages including basal cells, outer root sheath, and bulge cells.

Using NBT/BCIP *in situ* hybridizations with wild type embryonic tissue, miR-205 was shown to be expressed in the skin epidermis, the hair follicles in the head region (including eye/cornea expression), the liver, and the forebrain.

In order to clarify the expression of miR-205 in those tissues, high quality RNA was isolated from skin, brain, heart, and lung from P10 mice both wild type and miR-205 knock out mice. These RNAs were used as templates in RT-qPCR reactions as described in Materials and Methods. Internal controls, let7a and sno25, were included (let7a and sno25 are endogenously expressed microRNA). The results were normalized to RT-qPCR experiments on RNAs isolated from knock out head skin samples. The results confirmed that miR-205 expression was highly abundant in skin tissue (head skin), whereas expression in the lung was minimal. This suggests that miR-205 is highly specific and abundant in the skin tissue.

Section 2: Luciferase Assay

In situ hybridization techniques determined that miR-205 is expressed in undifferentiated cell types in embryonic and adult skin tissue. To incorporate miR-205 in regulatory pathways involving stem cell differentiation and function, investigation of the promoter region is necessary. Promoter regions are important DNA sequences that drive the expression of various genes and microRNA. The location of miR205's promoter will be useful in determining how this microRNA is regulated.

The UCSC Genome Browser and ChIP-Seq data were used to identify possible DNA sequences that might contain high promoter activity (Figure 3.16 and 3.17). MiR-205 is located in an exon of AK014513, an expressed sequence tag (EST) that has no recorded function (UCSC Genome Browser). Interestingly, miR-205 is located in a region flanked by 270KB that contain no other annotated genes. In addition, there is minimal evolutionary conservation scores several KB upstream of miR-205's transcriptional start site. The DNA flanking miR-205 has many regulatory elements (open reading frames, stop codons, introns, etc.) that could potentially

inhibit the presence of these surrounding sequences. This suggests that the miR-205 gene does not get translated and is positioned in the genome to insure transcription and processing into a mature microRNA.

Conventional promoters are located upstream of the transcription start site where various transcriptional machinery factors can be recruited to initiate transcription. Potential promoters for miR-205 were isolated from DNA upstream of the miR-205 gene. The promoter activity for miR-205 was hypothesized to be relatively similar to that of miR-203, which is high in keratinocytes isolated from mice. MiR-203 has a conventional promoter region, so it was thought that miR-205 would as well since both of these microRNAs are abundantly expressed in skin cell lineages.

Three pGL3 constructs were made with different DNA sequences trying to find the DNA regions responsible for driving miR-205's expression. These constructs were transfected into keratinocytes, after 48 hours luciferase activity was measured.

Construct A included several KB upstream of the transcriptional start site and DNA into the second exon right up to the miR-205 gene. Luciferase assays were used to determine the promoter activity of this construct. Promoter activity was normalized to the pGL3 basic construct, which lacked a promoter for the luciferase enzyme. Construct A showed a 5.6fold increase in promoter activity when compared to pGL3 basic. The expected promoter activity was hypothesized to be similar to positive controls, pGL3 control and pGL3-203, assuming miR-205 had a conventional promoter region. The relative fold change in luciferase expression between pGL3 control and pGL3 205 A was 290 demonstrating that the DNA in construct A did not have strong promoter activity.

Another promoter assay showed that construct B does not drive the expression of the luciferase gene. The relative fold change in luciferase activity between pGL3 basic and pGL3 205B was -.16. The activity of construct B suggests that this DNA may inhibit the expression of miR-205. Possible reasons for this DNA segment having a negative affect on the luciferase activity may be due to the interrupted intron in this sequence. Construct B contains DNA upstream of the transcriptional start site through the first intron. It is possible that the fragmented intron gets transcribed and represses activity of luciferase product. The DNA in construct B contains three open reading frames in the intron fragment. With each open reading frame, there is usually a stop codon downstream. If the intron is not spliced, these stop codons could potentially inhibit the translation of the luciferase gene, thus reporting no luciferase activity. However, this could also be experimental error. A repeated luciferase assay using construct B would be informative.

In the following assay, both construct A and C were tested to compare their promoter activities. Construct C included DNA immediately upstream of the transcriptional start site for miR-205. PGL3 205C showed minimal expression, 8.7 fold, over pGL3 basic. This implies that the region of DNA in construct C could have minimal promoter activity. Construct A showed similar luciferase activity, 10 fold over basic, thus construct A had 1.3fold expression over construct C. Both constructs show minimal activity relative to pGL3 control.

To determine if the minimal luciferase activity in constructs A and C are genuine, another luciferase assay was conducted in 293T cells rather than keratinocytes. Construct C was transfected into human embryonic kidney cells (293T cells, also referred to as BOC cells). The 293T cells have minimal to no miR-205 expression; (Yi, personal communication) thus the promoter activity for miR-205 in these cells should be null. PGL3 205C had minimal activity in

these cells, 12.8fold activity of pGL3 basic, similar to the previous luciferase assays. This experiment proves that there may be minimal miR-205 expression in these cells as well as demonstrating that constructs A and C are minimally active in tissues that do not have high miR-205 expression. Unfortunately it is not accurate to associate the promoter activity with the level of transcription of a gene. Some transcripts may be more stable and therefore do not need additional promoter activity. Thus, from this assay we can only conclude that the isolated promoter regions for miR-205 are minimally expressed in cells that have high and low expression of miR-205.

These results suggest that the region upstream of the transcriptional start site does not have strong promoter activity. There is some promoter activity however it was much less than expected. The promoter, or other enhancing elements, may be located elsewhere. There is about 500KB surrounding miR-205 without any other genes. This suggests that there may be important sequences in at a large distance from the transcriptional start site. It is possible for DNA further upstream of miR-205 to loop around and act as enhancing elements or essential promoter sequences. Therefore, constructs A and C do have minimal promoter activity, however since it is less than expected it is hypothesized that the true promoter and enhancer regions are located in the DNA surrounding miR-205.

Section 3: Conclusion

MicroRNAs are small non-coding RNAs that are present in many tissues and serve a wide variety of functions including stem cell regulation. It is known that microRNAs have differential expression in mouse skin making this an ideal system to study the role of micro RNAs in the differentiation of stem cells. Understanding microRNA expression can help elucidate their role in the maintenance and differentiation of skin and hair follicle stem cells. An

integral part of exploring microRNA function, is determining their distinct location and expression pattern in cell lineages. The microRNAs: miR-203, miR-143, miR-125b, and miR-205, have different expression patterns in epithelial tissue, which may suggest they have different functions in those cells. MiR-205 is expressed in differentiated cell lineages, suggesting that it may function by either promoting "stem-ness" or inhibiting differentiation.

Characterizing the promoter region of miR-205 is essential to understanding how this microRNA is transcriptionally regulated and can help lead to identifying possible regulatory factors that interact with this promoter. This microRNA could be implicated in multiple cellular mechanisms that control the fate of stem cells. The results indicate that miR-205 does not have a conventional promoter region located near the transcriptional start site. The promoter activity surrounding the transcriptional start site was much less than expected and it is therefore predicted to be located within a large region of DNA upstream of miR-205. Finding the promoter region will provide data for further investigation into the regulation of miR-205. Understanding where microRNAs are expressed and how they are regulated are important milestones that can be used to discover unknown networks of stem cell regulation.

Chapter 5: References

Bentwich, I., Avniel, A., Karov, Y., Aharonov, R., Gilad, S., Barad, O., Barzilai, A., Einat, P., Einav, U., Meiri, E.*, et al.* (2005). Identification of hundreds of conserved and nonconserved human microRNAs. Nat Genet *37*, 766-770.

Bostjancic, E., and Glavac, D. (2008). Importance of microRNAs in skin morphogenesis and diseases. Acta Dermatovenerol Alp Panonica Adriat *17*, 95-102.

Choi, P.S., Zakhary, L., Choi, W.Y., Caron, S., Alvarez-Saavedra, E., Miska, E.A., McManus, M., Harfe, B., Giraldez, A.J., Horvitz, H.R.*, et al.* (2008). Members of the miRNA-200 family regulate olfactory neurogenesis. Neuron *57*, 41-55.

Chomczynski, P., and Sacchi, N. (2006). The single-step method of RNA isolation by acid guanidinium thiocyanate-phenol-chloroform extraction: twenty-something years on. Nat Protoc *1*, 581-585.

Corcoran, D.L., Pandit, K.V., Gordon, B., Bhattacharjee, A., Kaminski, N., and Benos, P.V. (2009). Features of mammalian microRNA promoters emerge from polymerase II chromatin immunoprecipitation data. PLoS One *4*, e5279.

Clape, C., Fritz, V., Henriquet, C., Apparailly, F., Fernandez, P.L., Iborra, F., Avances, C., Villalba, M., Culine, S., and Fajas, L. (2009). miR-143 interferes with ERK5 signaling, and abrogates prostate cancer progression in mice. PLoS One *4*, e7542.

Cordes, K.R., Sheehy, N.T., White, M.P., Berry, E.C., Morton, S.U., Muth, A.N., Lee, T.H., Miano, J.M., Ivey, K.N., and Srivastava, D. (2009). miR-145 and miR-143 regulate smooth muscle cell fate and plasticity. Nature *460*, 705-710.

Dogini, D.B., Ribeiro, P.A., Rocha, C., Pereira, T.C., and Lopes-Cendes, I. (2008). MicroRNA expression profile in murine central nervous system development. J Mol Neurosci *35*, 331-337.

Elia, L., Quintavalle, M., Zhang, J., Contu, R., Cossu, L., Latronico, M.V., Peterson, K.L., Indolfi, C., Catalucci, D., Chen, J.*, et al.* (2009). The knockout of miR-143 and -145 alters smooth muscle cell maintenance and vascular homeostasis in mice: correlates with human disease. Cell Death Differ *16*, 1590-1598.

Greene, S.B., Gunaratne, P.H., Hammond, S.M., and Rosen, J.M. A putative role for microRNA-205 in mammary epithelial cell progenitors. J Cell Sci *123*, 606-618.

Kim, V.N., Han, J., and Siomi, M.C. (2009). Biogenesis of small RNAs in animals. Nat Rev Mol Cell Biol *10*, 126-139.

Lee, Y.S., and Dutta, A. (2009). MicroRNAs in cancer. Annu Rev Pathol *4*, 199-227.

Muller-Rover, S., Handjiski, B., van der Veen, C., Eichmuller, S., Foitzik, K., McKay, I.A., Stenn, K.S., and Paus, R. (2001). A comprehensive guide for the accurate classification of murine hair follicles in distinct hair cycle stages. J Invest Dermatol *117*, 3-15.

Takanabe, R., Ono, K., Abe, Y., Takaya, T., Horie, T., Wada, H., Kita, T., Satoh, N., Shimatsu, A., and Hasegawa, K. (2008). Up-regulated expression of microRNA-143 in association with obesity in adipose tissue of mice fed high-fat diet. Biochem Biophys Res Commun *376*, 728-732.

Valencia-Sanchez, M.A., Liu, J., Hannon, G.J., and Parker, R. (2006). Control of translation and mRNA degradation by miRNAs and siRNAs. Genes Dev *20*, 515-524.

Wang, Y., Medvid, R., Melton, C., Jaenisch, R., and Blelloch, R. (2007). DGCR8 is essential for microRNA biogenesis and silencing of embryonic stem cell self-renewal. Nat Genet *39*, 380-385.

Williams, A.E. (2008). Functional aspects of animal microRNAs. Cell Mol Life Sci *65*, 545-562.

Yi, R., and Fuchs, E. MicroRNA-mediated control in the skin. Cell Death Differ *17*, 229-235.

Yi, R., O'Carroll, D., Pasolli, H.A., Zhang, Z., Dietrich, F.S., Tarakhovsky, A., and Fuchs, E. (2006). Morphogenesis in skin is governed by discrete sets of differentially expressed microRNAs. Nat Genet *38*, 356-362.

Yi, R., Poy, M.N., Stoffel, M., and Fuchs, E. (2008). A skin microRNA promotes differentiation by repressing 'stemness'. Nature *452*, 225-229.

Zhang, L., Stokes, N., Polak, L., and Fuchs, E. Specific MicroRNAs Are Preferentially Expressed by Skin Stem Cells To Balance Self-Renewal and Early Lineage Commitment. Cell Stem Cell *8*, 294-308.

Chapter 6: Appendix

Section 1: Molecular Cloning

Construct A:

HindIII and Xho1 Digestion: 1Kb+ ladder run on .7% agarose gel

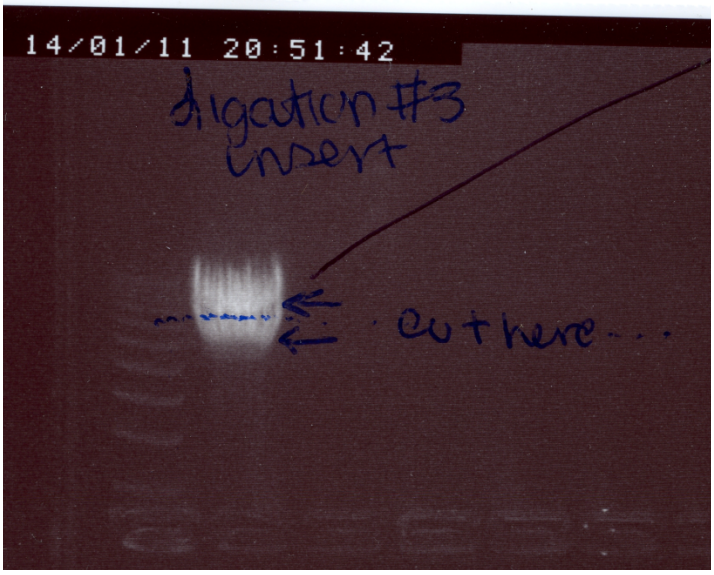

Construct A: Digested from *Plasmid #14 205 Final Targeting*:
Cut with HindIII and Xho1
Lane 1= 1Kb+ ladder
Lane 2=HindIII and Xho1 digest
Ideal band size:
HindIII and Xho1= 8.3Kb and 5.4Kb

The top band was cut out and purified. It was then ligated into pGL3 Basic. This insert was 8.5Kb

PCR Screen for correct orientation: 100bp ladder run on 1.5% agarose gel

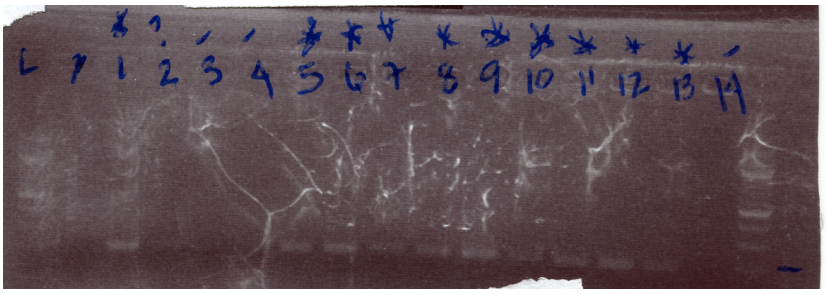

Construct A: PCR Screen with primer RY130pGL3Con400 and P1 205
Colonies were isolated that contained potential Construct A (#1-14)
Lane1=100Bp ladder
Lane 16= 100Bp ladder
Positive colonies=1,5,6,7,8,9,10,11,12,13
Ideal band size=200bp

Two colonies (#1, #9) with Construct A were then digested by restriction enzymes to verify the construct is the correct size: 1Kb+ ladder run on .7% agarose gel

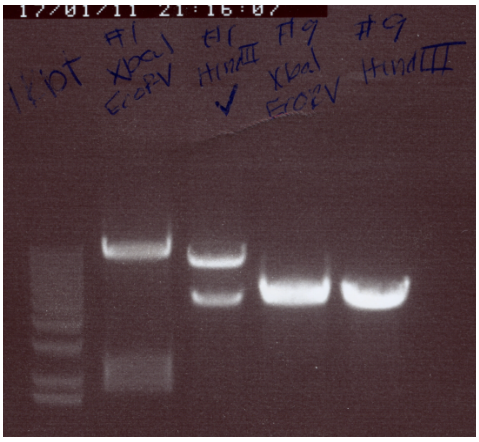

Construct A: #1 and #9 were cut with:
Xba1/EcoRV(X&E) and HindIII (H)
Lane 1= 1Kb+ ladder
Lane2= Construct A Colony #1 (X&E)
Lane 3= Construct A Colony #1 (H)
Lane 4= Construct A Colony #9 (X&E)
Lane 5= Construct A Colony #9 (H)
Ideal band sizes:
H&E= 9.38Kb and 3.74Kb
H= 8.5Kb and 4.8Kb

Construct A colony #1 was then digested again for further verification: 1Kb+ladder Run on a .7% agarose gel

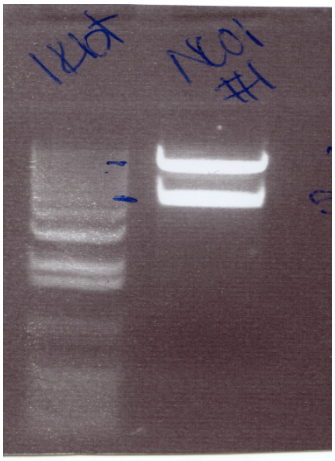

Construct A: colony#1 digested with Nco1
This cut will cut once in pGL3 near the 3' end of the insert and once in the insert.
Lane 1= 1 Kb+ ladder
Lane 2= Construct A colony #1 Nco1
Ideal band size:
Nco1= 8.5Kb and 4.5 Kb

Construct B:
Primers were for a smaller insert further upstream in hope to exclude open reading frames. PCR amplified the insert from *Plasmid #14 205 Final Targeting* with 10% DMSO and HF buffer: 1 Kb+ ladder run on .7% agarose gel

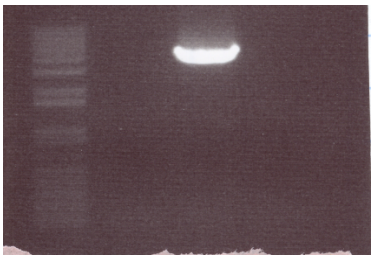

Construct B: PCR product = new insert
Lane 1= 1Kb+ ladder
Lane 2= negative control- no template
Lane 3= template- *Plasmid #14 205 Final Targeting*
Lane 4= template= genomic DNA
Ideal band size = 3.562 Kb

The new insert was Digested with HindIII and Nhe1 to be ligated into the multiple cloning site in pGL3. pGL3 Basic was also cut with HindIII and Nhe1. They were run on a .7% gel to verify there were no other unexpected cuts.

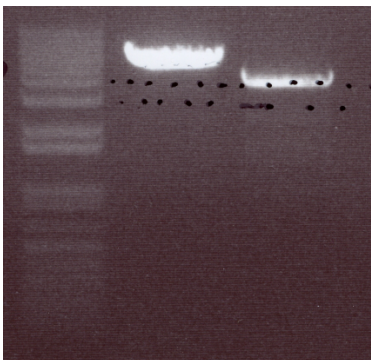

Construct B: Verification of insert and pGL3 pre-ligation
Lane 1= 1Kb+ ladder
Lane 2= pGL3 Basic cut with HindIII and Nhe1
Lane 3= Insert cut with HindIII and Nhe1
Ideal band sizes:
pGL3 Basic= 4.8Kb
Insert= 3.5Kb

The insert was ligated to pGL3 basic and transformed to Jm109 cells. Colonies were selected and verified with further restriction enzyme digestions. One negative colony (no insert was ligated) and three potential positive colonies labeled #1,2, and, 3 were selected.

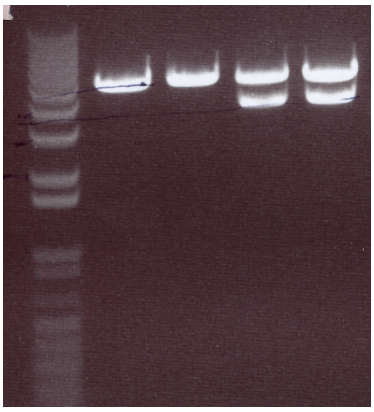

Construct B: Digestion verification for correct size of construct B. Digested with HindIII and Nhe1.
Lane 1= 1Kb+ ladder
Lane 2= negative colony
Lane 3= colony #1
Lane 4= colony #2
Lane 5= colony #3
Lane 6= colony #4
Colonies #3 and 4 were positive for the proper insert
Ideal band sizes= 4.8Kb an 3.5 Kb

Construct C:

Primers were made for a smaller insert starting at the transcriptional start site. PCR amplified the insert from *Plasmid #14 205 Final Targeting* with 10% DMSO and HF buffer: 1 Kb+ ladder run on .7% agarose gel

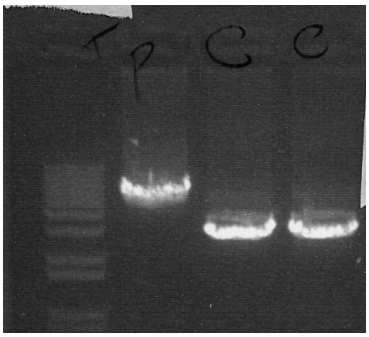

Construct C: PCR product = new insert
Lane 1= 1Kb+ ladder
Lane 2= DISMISS- not for this experiment
Lane 3= PCR product
Lane 4= PCR product repeat
Ideal band size = 2.7 Kb

The new insert was Digested with HindIII and Nhe1 to be ligated into the multiple cloning site in pGL3. pGL3 Basic was also cut with HindIII and Nhe1. They were run on a .7% gel to verify there were no other unexpected cuts.

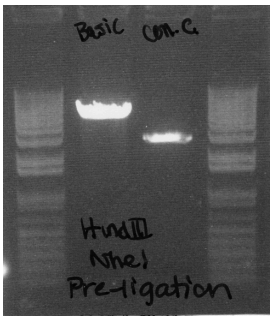

Construct C: Verification of insert and pGL3
pre-ligation
Lane 1= 1Kb+ ladder
Lane 2= pGL3 Basic cut with HindIII and Nhe1
Lane 3= Insert cut with HindIII and Nhe1
Ideal band sizes:
pGL3 Basic= 4.8Kb
Insert= 2.7Kb

The insert was ligated to pGL3 basic and transformed to Jm109 cells. Colonies were selected and verified with further restriction enzyme digestions. One negative colony (no insert was ligated) and three potential positive colonies labeled #1,2, and, 3 were selected.

Construct C: Digestion verification for correct size of construct C. Digested with HindIII and Nhe1.
Lane 1 and 11= 1Kb+ ladder
Lane 2= negative colony
Lane 3= colony #1
Lane 4= colony #2
Lane 5= colony #3
Lane 6= colony #4
Lane 7= colony #5
Lane 8= colony #6
Lane 9= colony #7
Lane 10= colony#8
Lane 11= colony #9
Lane 12= colony #10

Colonies #2,5,6,7,8,and 10 were positive for the proper insert
Ideal band sizes= 4.8Kb an 2.7 Kb

Section 2: In Situ Hybridization Trouble Shooting

Fluorescent In Situ Hybridization Trouble Shooting Table for microRNA 205

Slide Condition	Theoretical Validation	Genuine Specific Signal	Observations
Negative Control:	No probe hybridized=No specific signal	NO	No signal, some non specific in the Stratum Corneum
Standard slide: 5 min Proteinase K 61 ° C Hyb Temp 1/5000 Anti-DIG POD 7 min TSA-FITC Amp	Conditions Outlined in protocol that should be working	YES	Specific signal present not as strong as 1/1000. Otherwise clean.
Proteinase K 10 min:+ Standard conditions	Allows more signal by breaking down of proteins	YES	Not too big of a difference.
Hybridization Temp= 56 ° C+ Standard conditions	Allows more hybridization, less stringent	YES	More background.
Anti-DIG POD: 1/1000 + Standard conditions	More recognition of DIG label	YES	High signal strength and high background, with picture modifications. Best condition
TSA-FITC Amplification time: 25 min + Standard conditions	longer time would allow HRP to react longer potentially giving more signal	YES	Not too big of a difference. More back ground with more time
TSA-FITC Amplification time: 15 min + Standard conditions	longer time would allow HRP to react longer potentially giving more signal	YES	Not too big of a difference. More back ground with more time

- New Anti-DIG POD
- Old 205 probe
- New FITC

Section 3: Helpful Diagrams

Figure 5.1.

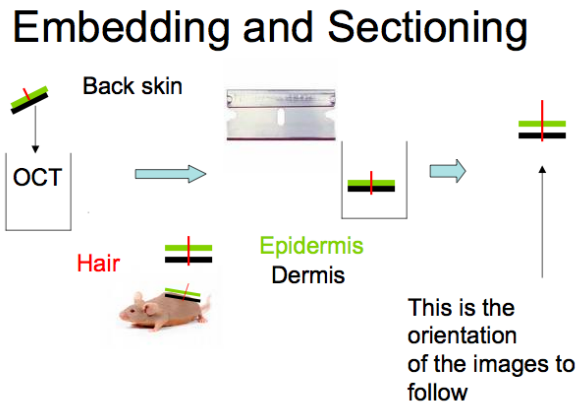

Figure 5.2

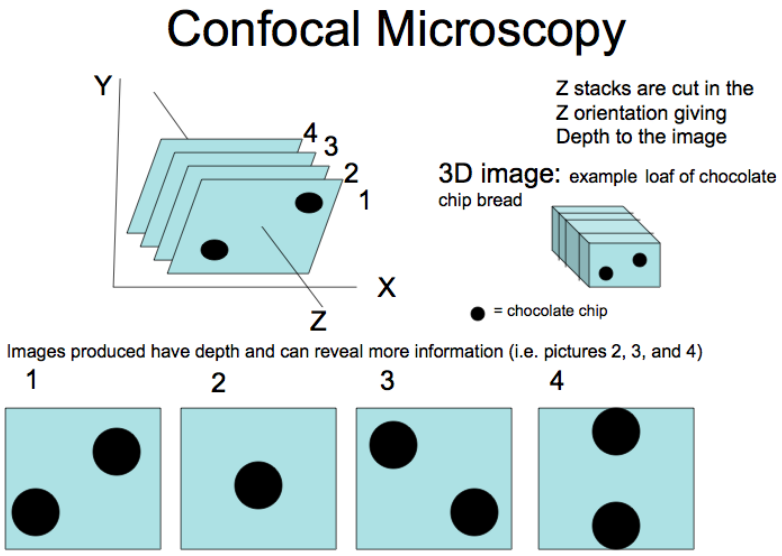

Figure 5.3

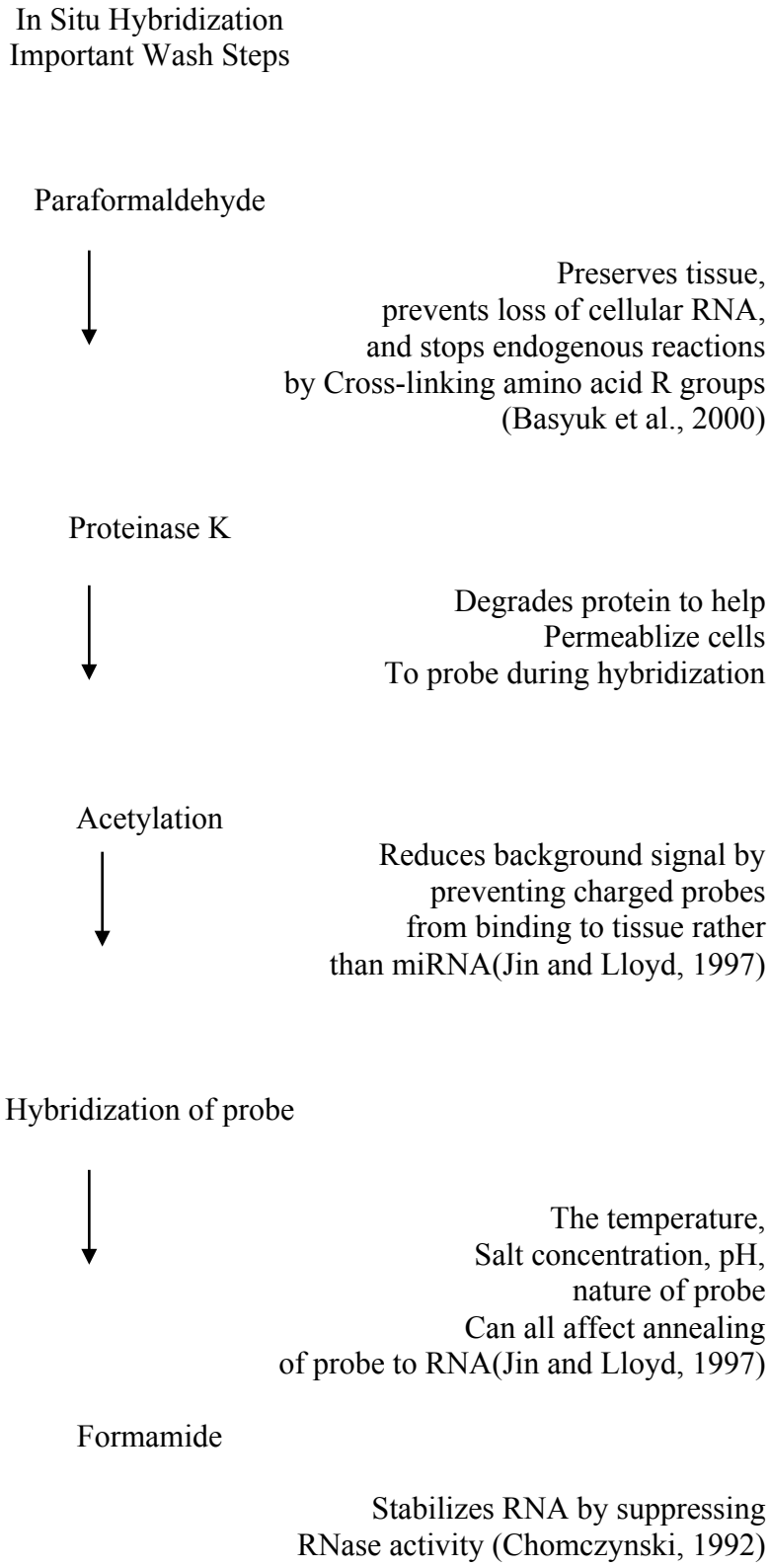
In Situ Hybridization
Important Wash Steps
Paraformaldehyde
Preserves tissue,
prevents loss of cellular RNA,
and stops endogenous reactions
by Cross-linking amino acid R groups
(Basyuk et al., 2000)
Proteinase K
Degrades protein to help
Permeablize cells
To probe during hybridization
Acetylation
Reduces background signal by
preventing charged probes
from binding to tissue rather
than miRNA(Jin and Lloyd, 1997)
Hybridization of probe
The temperature,
Salt concentration, pH,
nature of probe
Can all affect annealing
of probe to RNA(Jin and Lloyd, 1997)
Formamide
Stabilizes RNA by suppressing
RNase activity (Chomczynski, 1992)

Basyuk, E., Bertrand, E., and Journot, L. (2000). Alkaline fixation drastically improves the signal of in situ hybridization. Nucleic Acids Res *28*, E46.
Chomczynski, P. (1992). Solubilization in formamide protects RNA from degradation. Nucleic Acids Res *20*, 3791-3792.
Jin, L., and Lloyd, R.V. (1997). In situ hybridization: methods and applications. J Clin Lab Anal *11*, 2-9.

Figrue 5.4.

NBT/BCIP Reaction Details

Product Details:

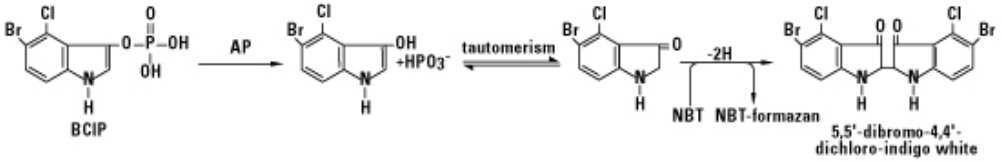

Chemical reaction of NBT and BCIP substrates with alkaline phosphatase. BCIP is hydrolyzed by alkaline phosphatase to form an intermediate that undergoes dimerization to produce an indigo dye. The NBT is reduced to the NBT-formazan by the two reducing equivalents generated by the dimerization. This reaction proceeds at a steady rate, allowing accurate control of the relative sensitivity and control of the development of the reaction.

1. Stuyver, L.J., et al. (2003). Antimicrob. Agents Chemother. 47, 244-254.

Figure 5.5.

Luciferase and Renilla Reaction Details

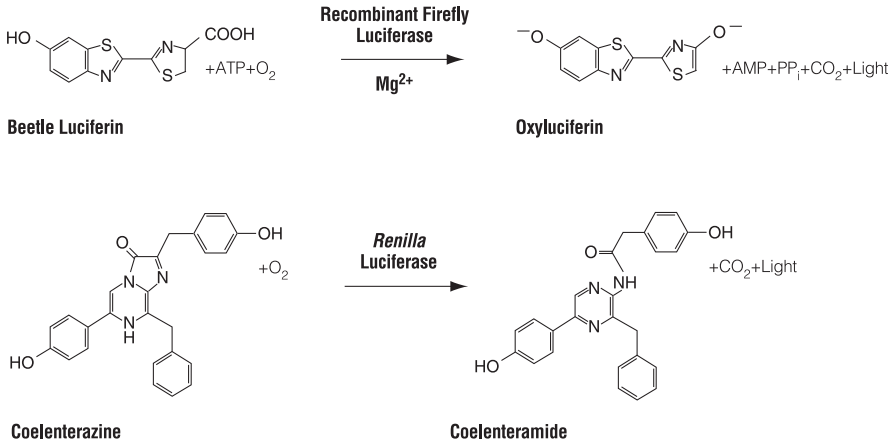

Image provided by: Promega Technical Manual:

Section 4: Further Explanations

A. Hair Follicle Cycling

There are three stages in hair follicle cycling: telogen, anagen, and catgen. Telogen is the resting phase between anagen and telogen. Anagen is the growth phase whereas catagen is the regression phase of the hair follicle. These cycles are important because they occur at different ages in mice and have different functions therefore different microRNA expression patterns. Below is a more detailed description of how to characterize the hair follicle stage and at what the different stages are present (Figure 1,2).

Figure 1 (Muller-Rover et al., 2001)

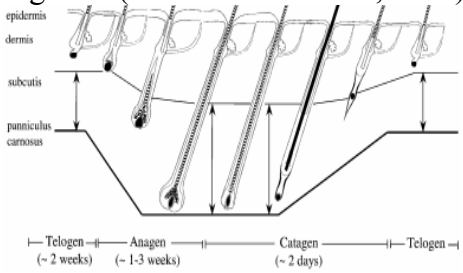

Figure 2 (Muller-Rover et al., 2001)

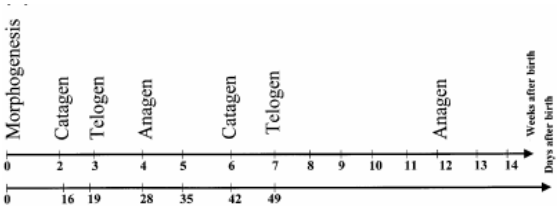

Telogen

Telogen is the resting stage before anagen begins. This stage in the cycle can first be identified at P19 right after the first catagen (Muller-Rover et al., 2001). This stage is usually presented first because it can serve as a way to orient readers before the first anagen. It is deceiving to think of the first anagen so late in the murine life because mice have hair before this age. The important aspect to consider is that the first hair growth is still part of hair follicle morphogenesis. Telogen is considered the resting phase because there are signs that there is no activation for growth. One of those signs is the size and shape of the DP cells residing below the hair follicle (HF). DP cells are mesenchymal cells thought to signal growth of the HF (Muller-Rover et al., 2001). In telogen, there is not a complex structure of differential cell layers in the hair follicle. As seen in Figure 3, there is no Inner Root Sheath (IRS). The IRS consists of multiple layers of differentiated keratinocytes medial to the hair shaft. The Outer Root Sheath (ORS) is present and is a barrier between the HF and the dermis.

Figure 3

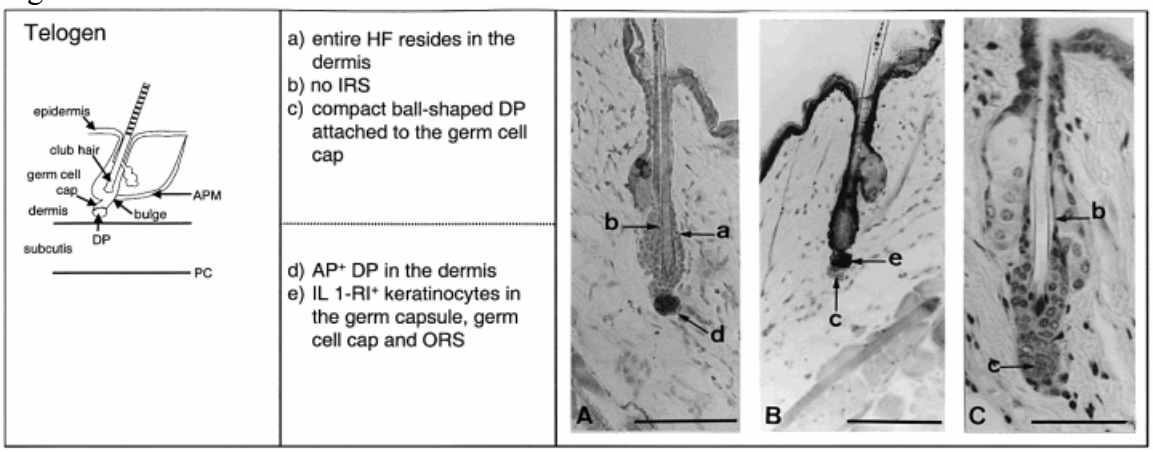

Anagen

Anagen is segregated into six stages. The first two stages are easily characterized because the HF is still completely surrounded by dermal fibroblasts just as in telogen. To distinguish between these two stages, it is important to look at the involvement of the DP with the germ cell cap and the size of the DP cluster. As anagen II becomes more predominant, the DP cluster enlarges and the germ cap starts to engulf the DP cells. Anagen III in more involved and is separated into three sub categories. The most important key to characterizing anagen III is the development and motility of the IRS. The IRS will assemble in anagen IIIa appearing as a cone of keratinized cells (Muller-Rover et al., 2001). The IRS will grow up until the bottom of the sebaceous gland. While the IRS is forming, another group of cells becomes identifiable as matrix cells. Matrix cells form the hair bulb and are known to be transit-amplifying cells. Matrix cells are highly proliferative and in the process of becoming differentiated into keratinocytes as they begin to travel up the IRS. Anagen progress in stages when the hair shaft enters the hair canal, and then when it emerges. See below figures for more detail.

Figure 4

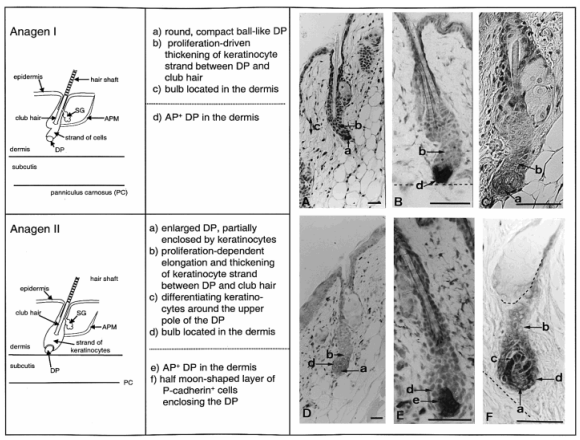

Figure 5

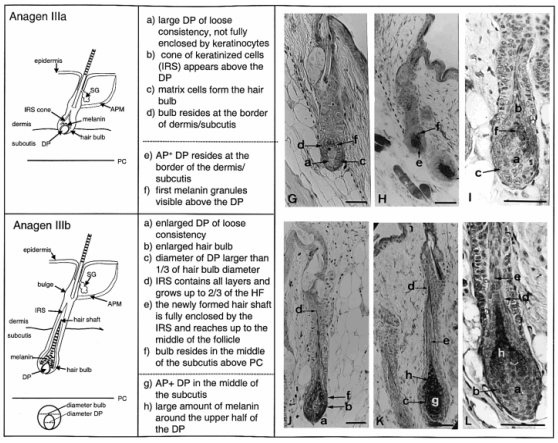

Figure 6

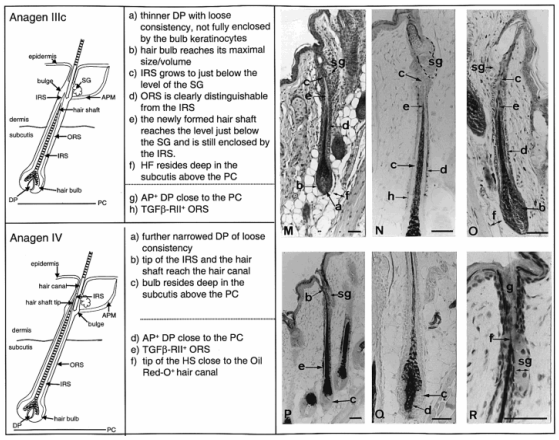

Figure 7

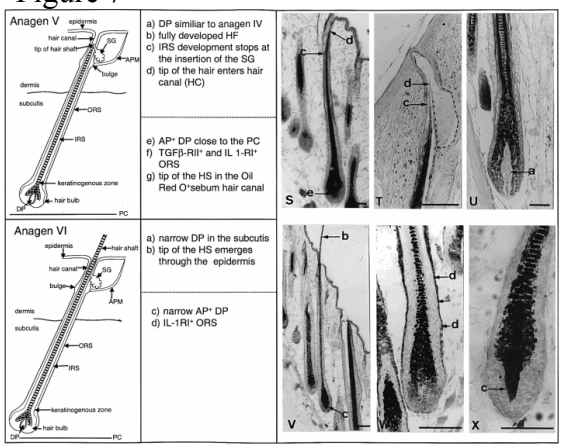

Catagen

Catagen is the destruction stage of the hair follicle. Catagen works in a similar reverse fashion compared to anagen. The first steps are to decrease the size of the hair bulb and decrease the surrounding surface area of the hair bulb and the DP cells. Once the hair bulb does no longer engulfs the DP cells, the length of the hair follicle decreases. It is lead by the regression of IRS cells. As the hair shaft regresses toward the surface epithelium, apoptosis increases at the bottom of the follicle allowing for the decreased length. Catagen is completed when the remaining IRS is below the sebaceous gland and when the hair germ capsule is in the dermis while the DP wells are directly below bordering the subcutis.

Figure 8

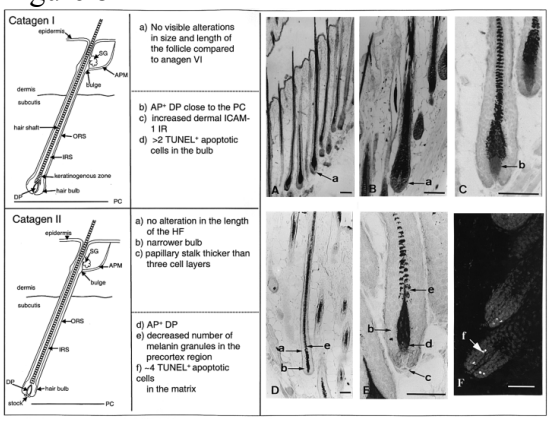

Figure 9

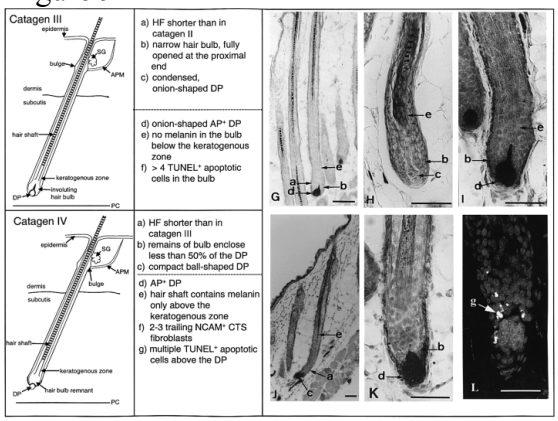

Figure 10

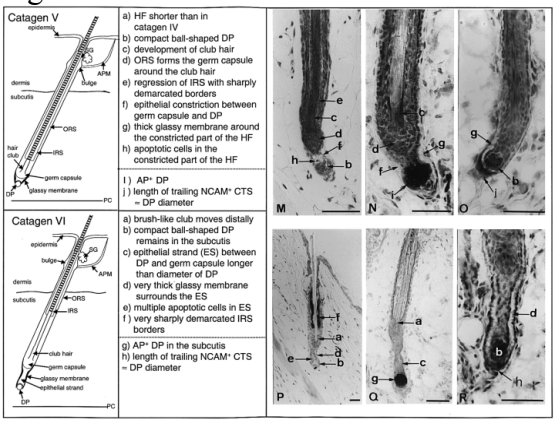

Figure 11

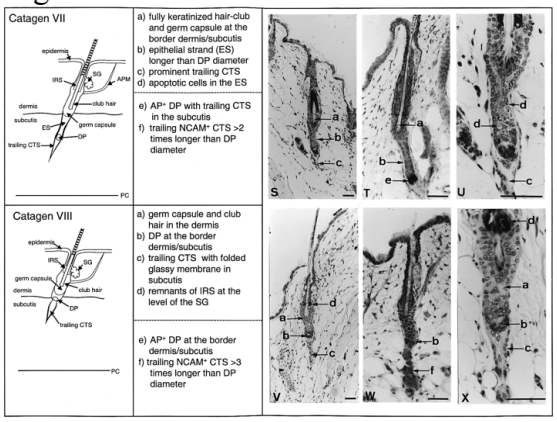

B. MicroRNA Function

When encapsulated within RISC, microRNAs function by targeting and silencing mRNA transcripts. A typical target region for miRNA would be in the 3' untranslated region (UTR) of the transcript. When mRNAs are transcribed, not all of the transcript will be translated into a protein. The regions that are not translated are thus referred to as UTR's. MicroRNAs are able to bind specifically to these regions to inhibit translation or promote degradation. MicroRNAs then reduce gene expression by four mechanisms (Valencia-Sanchez et al., 2006). See Table 1.

Table 1

Mechanism	Function
Site Specific Cleavage	MicroRNA seed sequences bind to target mRNA causing cleavage.
Translational Inhibition via RISC	RISC is able to inhibit translational initiation factors. The kinetics of RISC vs. translational machinery determine rate of inhibition.

Processing Bodies	This cellular organelle degrades mRNA that is sequestered away from ribosomes by microRNA, decreasing gene expression.
Adenine/Uricile Regulatory Sequence	This is a slicer/Ago2 independent pathway what is marked by adenine and uricile rich sequences.

Site Specific Cleavage: This mechanism involves the endonucleatic cleavage of mRNA. Essentially, when the miRNA binds to the 3' UTR of the target mRNA, specific sequences in the newly formed base pair between miRNA and the mRNA can trigger cleavage of the mRNA. Generally speaking, there are two key regions of the miRNA to consider when binding to the mRNA. The 5' end of the miRNA contains a five nucleotide sequence located between the second and seventh nucleotide in the 22-23nt miRNA (Valencia-Sanchez et al., 2006). This is called a "seed sequence." This region is thought to be specifically important for most, if not all, miRNA because this location has been highly conserved though evolution. The end, or 3' region, of the miRNA is associated with the destabilizing and degrading of the target mRNA. There are specific sites in this region that act as cleavage sites, for example, the 10^{th} and 11^{th} nucleotide region that acts as a marker for endonuclease activity. When mi-RNA is properly base paired with the target mRNA, the cutting and degrading activity of this class of enzymes is directed toward the middle of the polynucleotide chain. The cleavage of the mRNA greatly destabilized and can start a cascade of nuclease activity resulting in decreased gene expression due to reduced mRNA translation into proteins. (Valencia-Sanchez et al., 2006).

Nucleases are a family of enzymes that cut and degrade nucleotide regions. In this case the endonuclease activity is directed toward the 3'UTR bound to miRNA. In order for this activity to occur, the base pairs between the miRNA and the mRNA need to be perfect. There are few exceptions. The cleavage activity also needs to be mediated by Ago2. Ago2 is the only Ago in its family that is able to mediate this cleavage activity.

Processing Bodies (P-Bodies): Similar to site-specific cleavage, mRNAs may be degraded by cellular organelles known as Processing bodies (P-bodies). P-bodies are cellular organelles that contain nucleases capable of degrading "unwanted" nucleotide sequences. MicroRNAs mediate the movement of mRNAs to these organelles. Gene expression is affected by microRNA function because transported mRNAs can be degraded in the P-Bodies, but are also simply just sequestered away from translational machinery. The ability of microRNA to alter gene expression is dynamic because the rate and impact of its regulation is largely dependent on the target and its importance in the cell. Therefore, it is important to look at the whole picture, not just the specifics of how the P-bodies degrade the nucleotides. The rate of translation is affected by the rate of entry and exit into the P-bodies because those mRNA are no longer viable for translation. Therefore, mechanisms that control the rate of mRNA entry into P-Bodies, such as miRNAs, are a critical component of the equation.

Translation Inhibition via RISC: MicroRNAs can directly inhibit translation of its target mRNA. The RISC complex has been shown to inhibit initiation factors needed for the start of translation (Valencia-Sanchez et al., 2006). Additionally, RISC can alter the course of mRNA fate. Options for free mRNA in the cytoplasm are 1) translation, 2) cleavage, or 3) degradation by P-bodies. Kinetics dictates which outcome option is implemented (Valencia-Sanchez et al., 2006). If the concentration of P-body associated RNA binding proteins (mRNPs) is greater than

translational machinery, the mRNA is more likely to be sent to the P-body. RISC is essential in this role because it helps mRNPs assemble while blocking initiation factors. Thus, the RISC complex is tilting equilibrium in the favor of reduced gene expression (Valencia-Sanchez et al., 2006).

Adenine/Uracil Regulatory Sequence (ARE): The last mechanism is a slicer independent pathway for mRNA decay. When other Ago proteins 1,3,or 4 assemble with miRNA and RISC, rather than Ago-2, the complex does not have the slicing activity that Ago2 associated complexes do. Rather, the high decay rate of mRNA has been correlated to an AU-rich (Adenine adenine and Uracileuracile) 3' UTR regulatory sequence (ARE) (Valencia-Sanchez et al., 2006). ARE's play a role in controlling the decay rate of mRNA. This ultimately alters the rate at which translation and protein production occur. Therefore, they play a role in reducing the amount of mRNA to be translated and thus reducing gene expression.